INFLUENCE OF ADDITION OF CARBON NANOTUBES ON RHEOLOGICAL PROPERTIES OF SELECTED LIQUID LUBRICANTS - A COMPUTER SIMULATION STUDY

ANJALI CHOPRA
AND SZYMON WINCZEWSKI

Faculty of Applied Physics and Mathematics, Gdansk University of Technology, Gabriela Narutowicza 11/12, 80-233 Gdansk, Poland

(received: 20 August 2020; revised: 7 October 2020;
accepted: 1 November 2020 ; published online: 5 December 2020)

Abstract: This work is motivated by the improvement of anti-friction properties of lubricants by addition of CNTs proved experimentally in literature. In particular, a methodology is developed to compute the shear viscosity of liquid lubricants (Propylene Glycol) based on Molecular Dynamics simulation. Non-Equilibrium molecular dynamics (NEMD) approach is used with a reactive force field ReaxFF implemented in LAMMPS. The simulations are performed using the canonical (NVT) ensemble with the so-called SLLOD algorithm. Couette flow is imposed on the system by using Lees-Edwards periodic boundary conditions. Suitable parameters such as simulation time and imposed shear velocity are obtained. Using these parameters, the influence of addition of 2 7 wt% CNTs to Propylene Glycol on its viscosity is analyzed. Results show that 3.2 million time-steps with a 0.1 fs time-step size is not sufficient for the system to reach equilibrium state for such calculations. With the available computational resources, a shear velocity of 5×10^{-5} Å/fs was observed to give viscosity value with approximately 43% error as compared to the experimental value. Moreover, the lubricant exhibited a shear thinning behaviour with increasing shear rates. CNTs enhanced the lubricant's viscosity by 100-190% depending upon the averaging method used for calculation.

Keywords: Nanotechnology, tribology, lubricants, rheology, propylene glycol, carbon nanotubes, non-equilibrium molecular dynamics.

DOI: https://doi.org/10.34808/tq2020/24.4/c

1. Introduction

1.1. Background

Machines are becoming more complex day by day and are able to perform compound tasks. However, mighty as the machine may be, the physical wear

and tear is inevitable. It may be delayed but cannot be eliminated. This motivates our present work which, in a broad spectrum, is meant to improve the efficiency of engines and delay the wear and tear of engine parts. An essential part of this improvement process is the lubricating oil.

Lubricating oils (lubricants) are organic substances used in machines to reduce friction, heat and wear. They can be synthetic or mineral based - synthetic lubricants are manufactured using synthetic hydrocarbons while mineral based lubricants (mineral oil) are extracted from crude oil. The latter are more popular due to their low cost. Depending on the usage, lubricants can be in the solid (dry lubricant) or liquid form.

A lubricant works by creating a physical barrier between two surfaces. This not only reduces the friction between them but also reduces heat generation as well as surface fatigue. Lubricants also serve other purposes such as power transmission, anti-corrosion layer, sealant for pistons and debris removal. The largest users of lubricants are marine, aviation and automotive industries.

A typical liquid lubricant remains in the liquid state for a wide range of temperatures. This means that the lubricant exhibits a high boiling point and a low freezing point. The lubricant must not break down at higher temperatures, otherwise it might cause unwanted effects such as sludge formation. This property is known as thermal stability. The lubricant must show oxidative stability (the tendency to combine with oxygen). Other important properties of a typical lubricant are the pour point, the flash point and demulsibility (the ability to release/separate from water). The lubricant must also have a high viscosity index (VI) which means that it should not be significantly affected by temperature changes. Viscosity is one of the most important properties of a lubricant. Lubricants are often classified based on their viscosity as the requirements vary from thin oils needed for high speed components to thick ones for high temperature and loads. Hence, a wide range of lubricants are available depending on the usage and their properties.

The properties of lubricants can be enhanced by using some additives. A typical liquid lubricant is composed of 90% base oil and 10% additives (additive concentration varies) to obtain the desired rheological properties. Some major families of additives include pour point depressants, corrosion inhibitors, VI improvers, friction modifiers, *etc.* These additives are very important from a tribological point of view. Micro- and nano-particles of Copper, Tungsten, Molybdenum, *etc.* are commonly added to lubricating oils to reduce engine friction [1]. Another such promising additives for enhancing the tribological properties are the carbon nanotubes (CNTs). Recent studies show a decrease in friction, wear and improvement in the load carrying capacity by enhancing the viscosity of the lubricant upon adding CNTs. There is plethora of experimental research work [1–9] in this area but a deeper understanding of the physio-chemical process behind this phenomena is necessary. Since the additives are of nano-scale, the underlying phenomena cannot be studied using experimental methods. Molecular Dynamics can

be used to explore the tribological behavior of the additive enhanced lubricants at nano-scale. MD can provide an atomisitic-scale snapshot of the anti-friction mechanism at play. At every time-step, information regarding every atom such as its position, velocity, forces, *etc.* can be obtained. This information can then be used to extract displacement of atoms, frictional and normal forces, chemical reactivity, *etc.*. Parameters such as concentration of additives, the type of CNTs - single or multi-walled, the size of CNT, *etc.* can be thoroughly studied. Moreover, mechanisms such as agglomeration of additives, rolling, sliding, *etc.* could be observed for several lubricant and additive combinations. Materials and conditions pertaining to near-zero friction (superlubricity) could be identified for a number of applications. Reactive interatomic potentials have been utilized by researchers not only to determine the friction and wear between lubricants and the surface but also to study reactions within lubricants. In order to simulate such a system, a reliable and robust methodology must be available within the MD framework to compute the rheological properties of liquid hydrocarbons accurately. This in itself is a big challenge and has been the area of research in computational nanotechnology for several decades [10–25]. The limited spatial and temporal scales are often the culprit for a large gap between simulation and experimental results. Even with the recent advances in computational tribochemistry, the simulations match with the experiments only at a qualitative level. Therefore, only a partial validation can be performed [10]. Needless to say, a rheological study must involve studying and validating several existing MD methods so as to accurately describe the lubricant's properties associated with anti-friction and wear.

1.2. Literature Review

In recent years, a shift of industries towards efficient and sustainable energy consumption has been observed. This shift has greatly motivated research work in the field of green fuels and lubricants as lubricant usage significantly reduces friction losses in machines with moving components. New lubricants and additives are developed in order to reduce the wear and increase the efficiency. This is done, in practice, by optimizing the rheological properties of lubricants by adding colloidal solid particles (known as nanoparticle friction modifiers) [7]. Some of these additives are Titanium dioxide, Copper nanoparticles, CNTs, *etc.* These modifiers, especially nanocarbon-based lubricant additives, have shown to enhance the tribological properties of liquid lubricants. Nanocarbon based lubricant additives are a great choice due to their chemical stability and desirable mechanical properties. They can be used in various forms such as nanodiamond, C60 fullerene, carbon nanotubes, graphene, graphite, *etc.* CNTs dispersed in lubricant oil have shown a micro bearing-rolling lubrication on rubbing surfaces. On high loading conditions, they were also observed to easily open to form graphene like layers which exhibited good lubrication [9]. The lubricating performance with several additives has been studied extensively in the literature using experimental methods [1–5, 26–28]. They not only studied the rheological properties of lubricants but also the stability and dispersion of additives in those lubricants.

The full potential of nano-additives, especially CNTs, has not yet been realized due to several parameters affecting the dispersion and stability of CNTs in lubricants. Therefore, it is essential to study the influencing parameters in order to analyze the rheological behavior of modified lubricants.

Jabbari *et al.* [16] reviewed the parameters affecting the shear viscosity of nanofluids such as the nanoparticle size, volume fraction, aggregation, nanofluid temperature, *etc.* They reported that the increasing particle size was found to decrease the shear viscosity of the nanofluid. This behavior was justified by the increase in the particle-base fluid interaction energy for smaller nanoparticles immersed in the base fluid.

Mary *et al.* [28] performed an experimental study on the influence of the CNT concentration, temperature and shear rate on the rheology of acid treated MWCNT-Propylene glycol. They reported a non-linear increase in viscosity of the nanofluid with an increase in the concentration of MWCNTs, possibly due to their high aspect ratio and clustering behavior. Moreover, they reported the shear thinning behavior (a decrease in viscosity with the increasing shear rate) of the nanofluid.

Kałużny *et al.* experimentally studied the optimal parameters associated with adding CNTs to a motor oil for a successful engineering application [1]. The dispersion of CNTs, CNT types (single and multi-walled), wt% of CNTs and their size were some parameters considered in this study. The dispersion of CNTs in motor oil was found to be influenced by the motor oil viscosity prior to CNT addition. For liquids with low viscosity such as gasoline or ethanol, ultrasonicating the samples containing CNTs was found effective in dispersing the CNTs (breaking the agglomerates of CNTs). For highly viscous fluids like lubricating oil, dispersion with ultrasonication seemed ineffective although it formed a stable colloidal system which made the re-aggregation process of CNTs rather slow. The CNT addition, MWCNTs in particular, led to a significant decrease in friction losses associated with the engine operation. They also reported that CNT addition within 1% of the mass of lubricating oil was applicable to engineering applications as more CNTs would simply clog the pump. In a more recent experimental study by the same author [26], a reduction in wear is also shown by addition of MWCNTs in lubricating oil by forming an anti-wear (AW) layer.

Even though, there are promising experimental results, a lack of fundamental understanding of the physio-chemical process at play plagues the scientific community. Hence, a computational approach on a molecular level is required. Using Molecular Dynamics, friction reduction phenomena upon addition of additives such as CNTs in lubricating oils may be explored. This research gap has lead to several computational studies on the rheological properties of lubricants, the additives and their behavior in mechanical systems [12, 17, 21, 23–25, 29–32]. It was observed that the existing MD methods were not well-equipped to handle rheological calculations. This was evident by the large error in the computed value of viscosity when compared to the experimental value. Since then, several

methods have been developed using both equilibrium and non-equilibrium approaches to MD. Some of these methods include the SLLOD method [18, 19, 22, 23], direct method [33] (with two movable walls, limiting/forcing fluid flow/shear), the Müller-Plathe rNEMD (reversible non-equilibrium Molecular Dynamics) algorithm [21, 25], the Green-Kubo formalism [29–32] and other variants of these methods.

Non-equilibrium methods, also known as the NEMD methods, have gained popularity to compute rheological properties of a fluid, especially, lubricants of various molecular structures. The NEMD methods developed by Hoover and Ashurst [34] in 1975, later improved by Evans and Morris [35] are more robust and intuitive than the EMD methods as they imitate the experiment of viscosity measurement for a given liquid. The NEMD methods use a perturbation scheme rather than relying on fluctuations of pressure and momentum as in the EMD methods. This enables the NEMD methods to compute the parameters of interest such as viscosity much faster than the EMD methods. Thus, they may be used to study the rheology of lubricants with additives for reducing friction and wear in engine components. The most popular of the NEMD methods is the SLLOD method along with the Lees-Edwards periodic boundary conditions (LEbc), essentially imposing a Couette flow on the system [18, 19]. These methods have been discussed in great detail in literature and applied to various systems [8, 10, 11].

Several aspects must be considered to obtain useful results about the macroscopic quantities such as the viscosity, using NEMD methods. These aspects include the size of the system, the accuracy of the force field used for describing inter-atomic interactions and the computational time to reach the required time scale for calculations. The system size for an NEMD simulation of a tribological nature ranges typically over thousands of atoms. Even using high performance computing (HPC) and simplest force fields, it is only ns or μs (in rare cases) time scales that might be accessible.

Classical force fields are unable to accurately describe bond breaking and formation which leads to erroneous calculation of rheological quantities [10]. Chemical reactivity may be simulated using quantum methods but the time-scale required for viscosity calculation is not accessible in this case. Therefore, a hybrid solution has been sought by researchers. Reactive force fields, such as ReaxFF [36, 37], are capable of solving such problems enabling us to dive deeper into the mechanisms involved in friction and the wear reduction properties of nanoparticles added to liquid lubricants.

ReaxFF in conjunction with NEMD simulations makes it possible to access timescales required for rheological calculations of nanofluids [36]. This force field has at its core the so-called 'bond order formalism' which can approximate reactivity in classical MD simulations by using parameters derived from quantum calculations. A reliable parameter set is the most crucial aspect of such simulations. Chenoweth *et al.* presented the parameters for hydrocarbon oxidation which has been extremely useful in reactive MD simulations [37, 38].

The published literature may be used as a guideline for the present work. However, Jabbari *et al.* [16] reported that there were fewer studies on shear viscosity as compared to studies concerning on thermal conductivity. Hence, more research work is required to be able to compute the shear viscosity of a liquid with precision. Moreover, rheological computation of liquid lubricants using ReaxFF has been studied to a lesser extent, especially, Propylene Glycol with CNT additives. This observation served as a major motivation of the present work, with the main theme being the development of a methodology for such calculations.

1.3. Scope of the work

This paper aims at creating a methodology for reliable calculation of viscosity of liquid lubricants - with and without additives such as CNTs. This is done using the Molecular Dynamics program LAMMPS [33] and a reactive potential ReaxFF [37]. The non-equilibrium Molecular Dynamics method (SLLOD method) will be used to investigate the rheological properties of the system and validated for organic liquids. Once validated, the methodology will be extended to perform a study on the influence of CNTs on the rheological properties of organic liquid lubricants. This constitutes the first step in understanding the mechanism behind the improvement of the anti-friction properties of lubricants with CNT additives.

2. Theoretical background

2.1. Molecular Dynamics

Molecular Dynamics is a simulation technique used to perform computer experiments. The term 'molecular' tells us that we are working on a molecular scale and the term 'dynamics' tells us that we are interested in a temporal evolution of interacting particles at this scale. This is done by integrating the particle equations of motion. In Molecular Dynamics, the particles are treated as classical Newtonian particles following the Newton's law:

$$\mathbf{F}_i = m_i \mathbf{a}_i \qquad i = 1, ..., N \tag{1}$$

where, N denotes the number of atoms in the system. m_i denotes the mass of the i-th atom, $\mathbf{a}_i = \mathrm{d}^2\mathbf{r}_i/\mathrm{d}t^2$ denotes its acceleration and $\mathbf{F}_i$ is the time dependent force acting upon the atom due to interactions with other atoms. This force is usually a function of the positions of other atoms in the system but may also be, in addition, a function of particle velocities in some cases. Summarizing the MD methods, it can be said that with given initial positions and velocities of the atoms, the subsequent evolution in time and space can be determined which makes it a deterministic method unlike the Monte Carlo method. It will therefore mimic a real system and behave as a computer experiment, obviously with errors caused due to approximations in the treatment of interactions, *etc.* The classical treatment of atoms ignores the transfer of heat between moving atoms as well as the free electron gas which might produce errors in the simulation of metals where heat conduction by electrons is significant. Knowing that systems obey quantum laws rather than classical ones at an atomistic level, one could

ask why not to use quantum methods? Why not solve Schrödinger's equation instead of Newton's equation? The answer to such questions becomes apparent when one studies the basis of classical approximation, *i.e.*, the de Broglie thermal wavelength which is defined as:

$$\Lambda = \sqrt{\frac{2\pi\hbar^2}{Mk_BT}} \tag{2}$$

where, M is the atomic mass and T is the temperature of the system. Classical approximation is valid for systems with $\Lambda \ll aQQ$, a being the mean nearest neighbor separation. Therefore, classical approximation is unsuitable for the motion of light particles such as He, H_2, D_2, Ne *etc.* Moreover, quantum effects become significant in any system with a sufficiently low T. This is due to the specific heat dropping below the Debye temperature [39].

Classical approximation is excellent for a wide range of materials, however, it poses several limitations in terms of the time scale and size of the system. MD simulations can be performed on a time scale of a few pico-seconds to several hundred nanoseconds for a system containing thousands or millions of atoms, but in reality, the time required to accurately compute a quantity of interest may not be achievable by simulation. Regarding the size of the system, although simulation of a very large system may not be feasible due to computational limitations, a system which is too small can also be problematic. The MD methods rely on averaging the thermodynamic quantities which depend on the size of the system as well as the time scale. They are more accurate ($A \to A_0$, where A is any thermodynamic quantity and A_0 is its experimental value) when averaged over a very long time ($t \to \infty$) and for a very large system ($N \to \infty$) known as the 'thermodynamic limit'. Therefore, the system size and time scale must be given a thoughtful consideration for simulating any system.

MD has its roots in statistical mechanics and time averages of the thermodynamic quantities are used to connect the microscopic to a macroscopic scale. The state of the system is defined by a set of parameters such as the temperature, pressure, number of particles *etc.* The thermodynamic properties are derived from these parameters and the equations that govern the system. The microscopic state of a system in MD is defined by the positions of atoms and the momenta and is considered as coordinates in the multidimensional vector space known as the *phase space*. This phase space has $6N$ dimensions for a system with N particles - $3N$ dimensions for position and $3N$ for the momenta of all the particles. A single point in this space describes the state of the system:

$$q = (\mathbf{r}_1, ..., \mathbf{r}_N, m_1\dot{\mathbf{r}}_1, ..., m_N\dot{\mathbf{r}}_N) \tag{3}$$

The 'potential' of the system also known as the heart of MD simulations is defined in this phase space as will be seen later. In the phase space, a collection of points

that satisfy a thermodynamic state is known as an *ensemble*. Trajectories generated as a result of an MD simulation lie within this space and belong to the same ensemble. It is essentially a collection of various possible microscopic states for which the macroscopic or thermodynamic state is identical. Several such ensembles exist with various characteristics. Some of these are NVE, NVT, NPT and μVT ensembles. The nomenclature is quite straightforward and easy to understand. N is the number of atoms, E is energy, T is temperature, P is pressure, V is volume and μ is the chemical potential. The various ensembles pertain to the conservation of the quantities described by the name of the ensemble. The NVE ensemble, also known as the micro-canonical ensemble, is a thermodynamic state characterized by a fixed number of atoms, a constant volume and a constant energy which corresponds to an isolated system. The NVT ensemble (termed as the canonical ensemble) corresponds to a fixed number of atoms, volume and temperature. The NPT ensemble corresponds to an isobaric-isothermal system and the μVT ensemble or the grand canonical ensemble corresponds to a fixed value of the chemical potential, volume as well as temperature.

The average of a thermodynamic quantity A in an MD simulation can be ensemble average denoted by $\langle AQQ\rangle_{\text{ensemble}}$ or time average denoted by $\langle AQQ\rangle_{\text{time}}$. The ensemble average is obtained by averaging the thermodynamic quantity over all possible microscopic states of the system corresponding to the same macroscopic state. The time average is obtained by averaging the thermodynamic quantity over the length of the simulation. The dilemma of which one to use is resolved by the *ergodic hypothesis* which states that the time average equals the ensemble average based on the idea that if the system is allowed to evolve indefinitely, then the system will eventually pass through all the possible states. Practically, the simulations must be sufficiently long so that the ensemble averages can be approximated by time averages.

2.1.1. Potential

A Molecular Dynamics simulation requires a good representative model of the physical system to describe the intra- as well as inter-molecular forces of the simulated system. An accurate calculation of these forces is crucial for a 'realistic' description of the system, especially since the aim of these simulations is to acquire information on the atomic level. Such a model in the form of a mathematical expression is known as a force field/potential energy function also termed as *potential* given by $U = U(\mathbf{r}_1,...,\mathbf{r}_N)$. It is a function of its particles coordinates and is translationally and rotationally invariant. A potential is usually a decomposable function and can be written as:

$$U = U_0 + \sum_{i=1}^{N} U_1(\mathbf{r}_i) + \underbrace{\sum_{i=1}^{N}\sum_{j>i}^{N} U_2(\mathbf{r}_i,\mathbf{r}_j)}_{2-\text{body}} + \underbrace{\sum_{i=1}^{N}\sum_{j>i}^{N}\sum_{k>j}^{N} U_3(\mathbf{r}_i,\mathbf{r}_j,\mathbf{r}_k)}_{3-\text{body}} + ... \qquad (4)$$

Two body potentials are the most common due to their simplicity but there are plethora of many-body potentials. Some of the commonly used potentials

are the Lennard-Jones Potential, CHARMM, AMBER, AMOEBA, Sutton-Chen, Stillinger-Webber potentials, *etc.* depending on their description and capability to mimic real systems. The 'realness' of the simulated system depends solely on the extent of ability of the inter-atomic force to describe the forces experienced by the nuclei of a real atom in the same configuration. Therefore, it must be chosen carefully for the simulated system [40, 41].

The forces are obtained by computing the gradient of the potential energy function in the following way:

$$\mathbf{F}_i = -\nabla_{\mathbf{r}_i} U(\mathbf{r}_1, ..., \mathbf{r}_N) \tag{5}$$

The force field consists of a description of the potential energy in an analytical form as a sum of bonded and non-bonded interactions. Bonding interactions include stretching, bending and torsion modes whereas non-bonding interactions include electrostatic and Van der Waals terms. A typical force field is of the form:

$$U_{\text{ff}} = U_{\text{str}} + U_{\text{bend}} + U_{\text{tors}} + U_{\text{vdw}} + U_{\text{el}} + U_{\text{cross}} \tag{6}$$

In the above equation, U_{cross} is a coupling between the other contributions and is often neglected. These energy contributions are parameterized for various systems and the parameters are derived from *ab initio* or semi-empirical approaches. Equation (6) in an expanded form looks something like this:

$$\begin{aligned} U = \sum_{\text{bonds}} \frac{1}{2} k_b (r - r_0)^2 + \sum_{\text{angles}} \frac{1}{2} k_a (\theta - \theta_0)^2 + \sum_{\text{torsions}} \frac{V_n}{2} [1 + \cos(n\phi - \delta)] + \\ + \sum_{\text{improper}} V_{\text{imp}} + \sum_{\text{LJ}} 4\epsilon_{ij} \left(\frac{\sigma_{ij}^{12}}{r_{ij}^{12}} - \frac{\sigma_{ij}^{6}}{r_{ij}^{6}} \right) + \sum_{\text{elec}} \frac{q_i q_j}{r_{ij}}, \end{aligned} \tag{7}$$

where the first term denotes the sum over all bonds, r_0 being the equilibrium bond length and r the bond length for every ij atom pair. The second term represents the energy contribution due to the angle bending, where θ and θ_0 denote are the actual and the equilibrium values of the considered valence angle. The contribution of torsional energy is represented by a cosine function, where ϕ is the torsional angle, δ is the phase, n determines the number of minima or maxima between 0 and 2π, V_n determines the height of the potential barrier. The term with V_{imp} describes the energy contribution due to out-of-plane motions. The Van der Waals interactions between any two pair of atoms are usually described by the 12-6 Lennard-Jones (LJ) potential where, σ_{ij} describes the value at which the potential becomes zero and ϵ_{ij} denotes the depth of well for the interaction between atoms i and j. The last term describes the electrostatic interactions, where q_i and q_j are the partial atomic charges of atoms separated by a distance r_{ij}. In equation (7), the contributions to potential energy due to bond stretching, angle bending, dihedral and improper torsions (first four terms) are the intra-molecular or local contributions and the terms with LJ and elec are the contributions due to repulsive and Van der Waals interactions (Lennard-Jones potential) and Coulombic interactions, respectively [40].

Typically, a single force field can not be used to describe various atomic systems, due to the varying complexities and nature of these systems. This degree of variation has led to extensive research and several inter-atomic potentials are available and are continuously developed to provide more accurate results. The simulation results depend heavily on the force field used and are evident in several examples from the literature such as melting of Aluminum [42]. The differences in the results may be drastic or may appear correct even though they are not. Several reasons for this issue were discussed by Becker *et al.* [41].

As the complexity of a system increases, a much more sophisticated description of potential energy is necessary. Typically, empirical potentials require parameters that are obtained by fitting experimental data or data obtained from quantum calculations. Therefore, they can produce reliable results only for the systems that were used to obtain the parameters. Most current empirical potentials are suitable only for systems in which the bonds remain within 75% of their equilibrium value [43]. This is why such potentials cannot be used for simulating reactivity. A bridging potential is required to overcome this drawback and some novel potentials which do not require bond information in the description of the system have been developed and constitute what is called *reactive potentials*. Reactive potentials belong to empirical potentials which allow the possibility of simulating chemical reactivity. The parameters for such a potential are derived from quantum calculations. Reactive potentials unfold the possibility of simulating longer timescales than accessible by quantum methods. This allows us to simulate phenomena such as diffusibility, solubility, *etc.* without the computational expense of a typical quantum method. One such force field is ReaxFF [37] which will be used in the present work and which is discussed in detail below.

2.1.2. ReaxFF

ReaxFF as the name suggests is a reactive force field which is capable of determining whether or not a pair of atoms is bonded, thereby eliminating the need for the user to pre-define connectivity between atoms. This implicit bonding description removes the need for expensive calculations based on quantum methods. Being able to simulate reactivity using computational resources of a classical method has unlocked several possibilities for computational biology as well as chemistry. It has been successfully utilized for simulations of atomic layer decomposition, catalysis, proton diffusion membranes, *etc.* [38]. The main feature of this potential is the transferability of elemental description across different phases. This means that while an element may behave differently in different phases, its mathematical description remains the same. Therefore, reaction at interfaces (solid, liquid and gas) can be simulated with ease and allows for species migration in the system. It works for both bond breaking and bond formation by using implicit treatment of electronic interaction. ReaxFF uses bond-order formalism and polarizable charge descriptions for effectively handling reactive and non-re-

active simulations, respectively. Its potential function can be decomposed into several energy contributions as follows:

$$U = U_{\text{bond}} + U_{\text{over}} + U_{\text{under}} + U_{\text{val}} + U_{\text{pen}} + U_{\text{tors}} + U_{\text{vdW}} + U_{\text{Coul}} + U_{\text{specific}} \tag{8}$$

where, U_{bond} is a continuous function of the inter-atomic distance between two atoms and accounts for the bond formation energy. U_{over} and U_{under} are correction terms for bonding energy based on over-coordination and under-coordination of each bond. This is based on the atomic-valence rules. U_{val} and U_{tors} is the energy associated with the 3-body valence angle strain and the 4-body torsional angle strain, respectively. U_{pen} is the energy penalty for bond-angle energy for special cases. U_{vdW} and U_{Coul} is the van der Waals interaction energy and the Coulomb interaction energy, respectively and it is calculated between all atoms, disregarding the bond order and connectivity between them. U_{specific} is the energy contribution from system specific terms which are explicitly specified to capture properties such as lone-pair, conjugation, hydrogen binding and C_2 corrections. These terms are mostly empirical terms with fitting parameters which are derived by optimizing against a training set containing data from quantum calculations. The details of these calculations are provided by Chenoweth *et al.* [37].

The basis of ReaxFF is the bond-order formalism which computes bond-orders at every time-step throughout the simulation, thereby allowing bond formation and bond breakage. The bond order is directly calculated from the inter-atomic distances using the formula:

$$\begin{aligned} \text{BO}_{\text{ij}} &= \text{BO}_{\text{ij}} + \text{BO}_{\text{ij}} + \text{BO}_{\text{ij}} \\ &= \exp\left[p_{\text{bo}_1}\left(\frac{r_{ij}}{r_0^{\sigma}}\right)^{p_{\text{bo}_2}}\right] + \exp\left[p_{\text{bo}_3}\left(\frac{r_{ij}}{r_0^{\pi}}\right)^{p_{\text{bo}_4}}\right] + \exp\left[p_{\text{bo}_5}\left(\frac{r_{ij}}{r_0^{\pi\pi}}\right)^{p_{\text{bo}_6}}\right] \end{aligned} \tag{9}$$

In the above equation, the bond order (BO) between a pair of atoms $i-j$ is computed, where the terms with r_0 are equilibrium bond lengths and p_{bo} terms are empirical parameters obtained from an elaborate curve fitting and vary with atomic species. Therefore, there are various implementations of ReaxFF in MD codes to suit specific systems. This bond-order formula is capable of accurately predicting the reaction barriers by using a long-range covalent bonding feature. This feature captures even the weakest of interactions (typically, 5 Angstrom but maybe extended) which are often seen in transition-state structures. Nevertheless, this feature may cause spurious bond characters between unbonded neighboring atoms due to which a correction term is added. Therefore, the bond order dependent terms such as bond energy and angle strains use the corrected bond order for calculations. ReaxFF computes bonded and non-bonded terms independently and does not transfer any information between the terms depending on the bond-order and the van der Waals and Coulombic terms. Coulombic terms are computed using a charge equilibration scheme which calculates partial atomic charges at each iteration. All the terms are calculated for all molecules present in the simulation in order to provide a wholesome description of the system. This

seemingly perfect force field to simulate everything from reactive to non-reactive systems has its flaws. The development of this force field along with its advantages and disadvantages has been discussed very thoroughly in the literature [38].

2.1.3. Initial structure

A simulation is started by creating a simulation box where N particles are placed with certain velocities. These will be the initial positions and velocities assigned to the particles. The structure thus created is called the initial structure. The initial structure of the system is an important aspect which cannot be overlooked as providing a good structure at the start of the simulation will lead to faster convergence. It can be created either from scratch or taken from a previously simulated system. To start from scratch, we create appropriate positions and velocity of the system to be simulated. To create an initial structure from scratch, several methods may be used based on the required target structure and the available computational resources. The random approach, lattice start and skew start are some of those methods. For simulation of solid structures, it is easy to create an initial structure as the expected structure is known from experiments. The lattice start is usually the way to go for crystal structures. However, it is more challenging to create a liquid structure or an amorphous one. 'Annealing' is an option often used where a crystal structure is created according to the density of the liquid and subjected to heat which would slowly change it to the desired phase. This method is very time consuming and leaves some crystalline remnants in the molten structure. The 'skew start' method is more handy in creating liquid and gaseous structures as it guarantees minimum separation without introducing periodicity [44]. This prevents what is called a 'group photo paradox'. We will focus on the random approach as it is the method used to create the initial structure in the present work as the system is a disordered one (liquid). This approach introduces randomness in the starting sample so as to have a non-zero net force on the atoms. This prevents atoms from sitting in the same position due to symmetry for the entirety of the run [45]. The velocities of the particles in the initial structure are also required for an MD simulation. The velocities may be taken from the Maxwell-Boltzmann distribution given by the equation:

$$f_{\mathrm{M-B}}(v) = 4\pi v^2 \left(\frac{m}{2\pi k_{\mathrm{B}} T}\right)^{3/2} \exp\left[-\frac{mv^2}{2k_{\mathrm{B}}T}\right] \tag{10}$$

where, k_{B} is the Boltzmann constant ($k_{\mathrm{B}} = 1.3806 \times 10^{-23}$ J/K). Since velocity is a vector, directions are also required and they are randomly drawn from a uniform distribution over a sphere. A 'good' initial structure is one where the potential energy is close to minimum and a 'bad' one is usually where the energy is far from minimum. A good structure is often obtained from a crystal structure or a lattice approach, and the latter is obtained typically from the skew start or other methods of generating the initial structure. There is a lot of excess potential energy in such systems and it is transferred to kinetic energy which translates

into rapid heating of the system. This may become uncontrollable and the system may explode rather quickly. Hence, we need a condition that would stabilize the system in the beginning and prevent it from exploding. This is known as *equilibration* and will be discussed next.

2.1.4. Equilibration

Every initial structure created may not necessarily be a good one, *i.e.*, one where the descriptors of the state of the system are not stationary (fluctuating around a fixed value). More often than not, the initial system is not a good representation of the system which we need to simulate. Moreover, in every MD simulation, a system is characterized by a certain value of density, pressure and temperature which are calculated for the system. These parameters need to be controlled in order to drive the system towards a desired state in a thermodynamic equilibrium. However, even the slightest changes in the state of the system can drive the system out of equilibrium, at least for a while. This means that the system parameters or thermodynamic quantities do not remain constant. They fluctuate around a fixed value but this value drifts slowly with time. These changes may be introduced when a new value is assigned to one of the parameters, causing a perturbation which disappears as the system attains a new equilibrium. These changes may also be introduced spontaneously, *e.g.*, when the system undergoes phase transition. Since, the aim of the MD simulation is to perform a 'computer experiment' and compute the desired values, these 'experiments' must be conducted after an equilibrium state has been reached. For a physical quantity, A, the equilibrium value A_0 is attained exponentially with time according to:

$$A(t) = A_0 + C\exp(-t/\tau) \tag{11}$$

where, A is averaged over a short time to remove the effect of instantaneous fluctuations but takes into account the long-term drift. τ is the *relaxation time* which may be of the order of hundreds of time steps or larger than the overall simulation time scale. Smaller values of τ allow us to see and measure the equilibrium value, however, for larger values, one can apply Equation (11) to estimate A_0.

During the equilibration, a system can be controlled artificially to stay at a certain temperature through *velocity scaling* or *force capping*. Due to artificial modification of velocities, the system does not follow Newtonian equations and discontinuous jumps in the phase space are observed. Therefore, we discard the simulations performed during equilibration and use the system thus obtained with the desired state parameters to run the computer experiments which is known as the *production run*.

2.1.5. Production run

The equilibrated system thus obtained is used for further simulations to achieve the required parameters and is called a *production run*. This part of the MD simulations is known as the 'computer experiment' and all other parts are necessary to set up this experiment. The desired quantities in MD

are computed at this stage and relevant information is extracted. This can be done visually by inspection in order to 'see' the behavior of the system using the available molecular visualization tools such as VMD [46], OVITO [47], PyMol [48], *etc.*

In many cases, visualization is not a very helpful tool due to a complex arrangement of atoms as well as the little information it provides by just looking at a system. As in experiments, probes are set to determine the values of certain parameters and the quantities of interest can be obtained using calculations. This is done by using *time-averaging* of the physical properties over the system trajectory whose information is contained in the phase space. The instantaneous value $A(t)$ of any quantity A is generally a function of the particle position, velocities and forces (the force required for pressure calculation using the Clausius virial function) as:

$$A(t) = f(\mathbf{r}_1(t),...,\mathbf{r}_N(t),\mathbf{v}_1(t),...,\mathbf{v}_N(t),\mathbf{F}_1(t),...,\mathbf{F}_N(t))$$

The average of this quantity is then obtained by:

$$\langle AQQ! \rangle = \frac{1}{N_T}\sum_{t=1}^{N_T} A(t) \tag{12}$$

where, t is the time step that runs from 1 to the total time steps N_T.

Though quantities that are of interest can be computed using the above averaging technique, the trajectories of the particles are unknown. To obtain them, the *finite-difference* approach is used to integrate the equations of motion, once the forces are calculated. An integrator is required for a continuous potential models as the motions of all particles are coupled and this 'many-body' problem cannot be solved analytically. The integration algorithm is also known as the 'engine' of an MD program. In these algorithms, time is discretized on a finite grid with Δt as the distance between consecutive points on the grid. The quantities are evaluated at a later time step $t+\Delta t$ using the positions and their time derivatives at time t. Thus, the system evolution can be obtained using an iterative procedure. Since these quantities can only be approximated using such integrators, they are not free from errors such as the *truncation errors* and the *round-off errors*. Of course, errors can be reduced by reducing the value of Δt since truncation errors dominate for large values of Δt. Round-off errors are due to the implementation of the algorithm and can be kept at a minimum by using the 64-bit precision.

Several algorithms exist for the integration using finite-difference methods in MD simulations. The common assumption is that the positions as well as the dynamic properties such as velocity, acceleration, *etc.* can be approximated using the Taylor series expansion. Some of the popular algorithms for a numerical solution of the equations of motion are the Verlet, Predictor-Corrector, Leap-frog and velocity Verlet algorithms. The last algorithm is used in the present calculations.

2.1.6. Periodic Boundary Conditions

A crucial step in MD simulations is to set up a system that truly represents the real system and that can be simulated with the given hardware capabilities. Often, the goal of MD simulations is to compute quantities (temperature, pressure, density, *etc.*) associated with a bulk or macroscopic sample. This prompts us to create as large a system as computationally feasible, however, the number of atoms N will always be negligible as compared to N in a macroscopic sample. Thus, the ratio between the surface atoms and the total number of atoms will be much greater than it would be in reality which would cause surface effects to be more pronounced than they should be. Moreover, we know that there will be less error and fluctuations in these quantities as the system approaches the thermodynamic limit ($N \to \infty$). Even though present day computers can simulate millions of atoms, simulations running for a few nanoseconds could require several CPU-days to complete. Therefore, an adequate system size must be chosen according to the available computational power. We should create the smallest possible system that will resemble the behavior of a full size system, even an infinite one. This can be done by using the appropriate boundary conditions for the simulated system. They can be periodic or non-periodic. A non-periodic boundary is used to simulate a finite system, but periodic boundary conditions are used to simulate a bulk phase.

The periodic boundary conditions (PBC) mimic an infinite bulk surrounding the created N-particle system. It allows us to perform simulations with a relatively small size of the system (small number of particles constituting the system). Here, the system is bounded but is free of walls. A *primary cell* with N-particles is surrounded by infinite identical copies or images which are known as *image cells* as shown in Figure 1. Hence, only the primary cell is simulated and macroscopic quantities can be extracted using an infinite-copy arrangement. Here, a wraparound effect is created which has two important aspects. One, that an atom leaving the primary cell through a particular boundary immediately enters the cell through the opposite boundary. The second, that the atoms lying within a fixed *cut-off radius* r_c of a boundary interact with the atoms in the neighboring image cell or near the opposite boundary of the primary cell. In this way, there are no physical boundaries, although the system is bounded. This wraparound effect is taken into consideration in all parts of the simulation - from creation of the initial structure to computation of interactions. A particle in such a primary cell located at a position r, practically, represents an infinite set of particles which are its images but only one constitutes the simulation. By doing so, surface effects are mitigated and the boundaries are eliminated. Although, one unrealistic effect seen as an effect of PBC is the enormous increase in the interacting pairs which does not happen when using short range potentials. This problem is solved using what is known as the *minimum image criterion* and simplifies the complexities introduced by PBC implementation in a program.

As everything in the world, PBC are not perfect and must have some flaws. Replicas or images of the principle cells make atoms in all images move in sync. This leads to artificial correlations between atoms and produces errors in the energy description. A *quasi-infinite* system is obtained using the PBC rather than an infinite one. There is also a lack of proper definition of the angular momentum under PBC, this leads to nonphysical frictional forces between images upon rotation of particles or the system. Moreover, errors in calculations occur for long-range interactions such as Coulombic forces as well as for systems with impurities or defect. A much bigger system surrounding the defects is needed to accurately simulate the system. Mixed boundary conditions are often used such as the slab boundary conditions or the wire boundary conditions to deal with such problems.

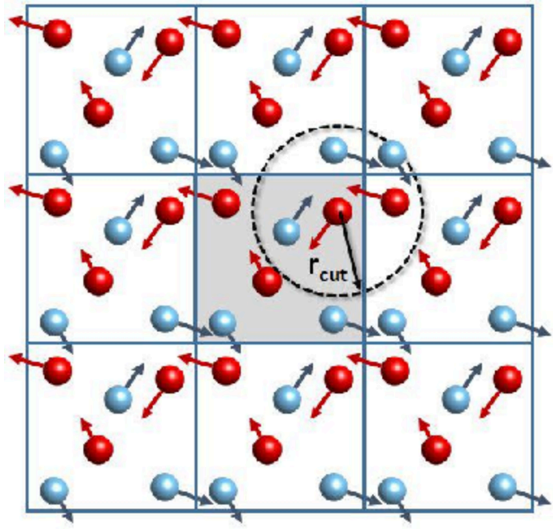

Figure 1. Periodic boundary conditions for a two-dimensional cubical box [49]

2.1.7. Minimum Image Criterion

When using PBC, a very obvious problem that occurs is that each particle i in the principle cell would interact with all images of particles $j_1, j_2, ..., j_N$ in the image cells. This would cause an unrealistic increase in non-bonded interactions and the terms associated with it in the potential function which is not justified for most potentials as they are short range potentials *e.g.*, the Lennard-Jones potential. The L-J potential decreases rapidly as the distance increases and at 2.5σ, it has only 1% of the value at σ. These interactions are truncated using the minimum image convention. In this convention, each atom in the principle cell basically sees only one image of every other atom and the forces are computed with the closest image or atom. The cut-off value r_c truncates all interactions beyond this radius and takes into account only the closest image as is shown

in Figure 1. There are certain guidelines that must be followed in order to implement the minimum image criterion with the PBC. An optimum value of r_c should be used. The cut-off value must be small enough to not have the same particle twice or that a particle in the principle cell sees its own image. Following this guideline for the upper limit, r_c should be no more than half the length of the cell in case of a cubic cell, and no greater than half the length of the shortest side for a rectangular cell. The value also depends on the potential used, whether it is short range or long range potential [50].

2.1.8. Neighbor Lists

By using minimum image convention, we are able to mitigate the problem that occurs with PBC but it still requires the program to calculate distances between every pair of atoms r_{ij} in the system in order to decide whether they lie within the cut-off radius to be able to contribute to the interaction energy. From a computational point of view, the calculation of $N(N-1)$ distances is very taxing and equivalent to calculating the energy itself. This can be solved by studying the nature of the system and determining how often the distances must be calculated. This is done by storing the positions of the atoms in an array which allows us to determine the neighbors of each atom without having to calculate the distance between every atom at every step. Such a neighbor list was first proposed by Verlet in 1967 and is known as the Verlet neighbor list [51].

The Verlet neighbor list stores all atoms within the cut-off radius as well as atoms which are slightly away from r_c. All r_{ij} are computed at once at the beginning of the simulation and the list of neighboring atoms is stored for each atom i. Then, r_{ij} is calculated only for the j atoms that are neighbors of i. The list is updated every k steps depending on the system - liquid atoms move more often than solid atoms (typically, 5-10 for liquids and 5000 for solids). We can specify the neighbor list refresh rate for the simulated system. The positions of atoms are stored according to the specified value of the refresh parameter during the course of the simulation. The list is updated when there is movement of atoms by more than Δr. In this way, r_{ij} is calculated every k steps and the neighbor list is updated. This method may cause energy jitter due to the fact that an atom which might be outside the cut-off radius when the list is refreshed may come inside the r_c before the next refresh. This may be eliminated by keeping atoms within $r_c + \Delta r$ in the list. It may also be done by keeping two lists instead of one where the list of close atoms is updated more often than the list of distant atoms. Of course, this is done at the expense of the system memory and the complexity still remains $O(N^2)$.

Another method which is very popular is the *Hockney's linked cells* method [52]. It avoids the calculation of all r_{ij} every once in a while by using a smarter approach. In this method, the simulation box is divided into *cells* with a prescribed length $l = r_c$. The atoms which lie within $r_{ij} \leq r_c$ then, must be in the same cell or the neighboring cells. In this way, we calculate r_{ij} only for atoms j that are in the neighboring cells of atom i if and only if we remember

the location of atoms with respect to the cells. This is easily done by calculating $(\lceil x_i/r_c \rceil, \lceil y_i/r_c \rceil, \lceil z_i/r_c \rceil)$ for atom i which is fast $\sim$ O(N). This method is not used in very small simulations due to a large overhead as it uses two arrays, one with N elements (atoms) and the other with M elements for the cells into which the system is divided where, typically, $N \gg M$.

The current implementations of MD employs a combination of both the Verlet list and Hockney's linked cells method. The neighbors are identified using Hockney's cells and the neighbors are stored in the form of the Verlet list. This combination eliminates the high computation penalty associated with the Verlet method in finding the neighbors as well as the large overhead in Hockney's methods for smaller systems.

2.2. Calculation Method

2.2.1. Viscosity

Viscosity is defined as the propensity of fluid to transmit momentum perpendicular to the direction of the momentum flow (shear). Physically, this means the resistance or fluid friction to the flow. A fluid is called highly viscous if there is a high fluid friction such as the flow of honey compared to water. Water in this case is less viscous because it flows easily. Hence, one may also call viscosity a drag force. Viscosity is a fundamental transport property which arises due to the transfer of momentum between layers of fluid (laminae) that move with different velocities. It describes the momentum dissipation in a fluid. There are two forms of viscosity namely:

- Absolute or dynamic viscosity or shear viscosity
- Kinematic viscosity

In simple words, dynamic viscosity describes the tangential force per unit area required to slide fluid laminae one over another and its SI units are N·s/m^2, Pa·s, or kg/m·s. It can also be expressed in Poise (1 P = 0.1 Pa·s). The kinematic viscosity takes into account the gravitational force by including the density term. In other words, the kinematic viscosity measures the fluid resistance to flow when there is no external force (except gravity) acting on it. Its SI units are Stokes (St) or Centistokes (cSt) after the Irish mathematician and physicist George Stokes. It can be measured experimentally using a viscometer or a rheometer. Dynamic viscosity measurements are used for non-Newtonian fluids (ketchup, toothpaste, blood, *etc.*) and kinematic viscosity measurements are often used for Newtonian fluids (water, oils, *etc.*). Newtonian and non-Newtonian fluids will be explained further in this section.

Measurement of viscosity is of great importance not only to scientists and engineers but also to laymen. As such, it is largely affected by factors such as the molecular structure of the fluid, external forces acting upon the fluid as well as the ambient conditions of the surroundings. The combination of these internal and external factors defines the flow behavior of a fluid. A substance with

strong inter-molecular bonds is highly viscous and resists any kind of deformation and therefore resists the motion between fluid layers *e.g.*, honey, butter, molten glass. Additionally, the conditions to which the flow is subjected also influence the flow – the temperature and the pressure of the surroundings. Viscosity is a kinetic property, and thus, the temperature determines the degree of motion of the molecules which in turn influences the flow behavior. In liquids, there is an inverse dependence of viscosity on temperature which is important in the automotive industry where lubricants subjected to lower temperatures in winter may show increased viscosity and cause problems while trying to start the engine of the vehicle. This is why, some additives and lubricants are added to fuels so that the engine should keep working even at much lower temperatures by changing the viscosity of the lubricant. However, in gases a direct relation is observed which is due to the increased collision rate of the molecules, hence, an overall reduced mobility at higher temperatures. Moreover, liquids subjected to extreme pressure show an increase in viscosity and although several models exist to describe this behavior, there is no consensus on a perfect model which makes the liquid phase much less understood than solids or gases.

In addition to the internal structure and ambient conditions, the external forces acting upon the fluid (known as shear stress) play a major role in determining the viscosity of the fluid. Considering a Couette flow where the fluid flows between two plates parallel to each other with one plate in relative motion to the other, the shear stress describes the stress applied to the fluid by the movement of the upper plate parallel to the surface of the plate.

$$\tau = \frac{F}{A} \tag{13}$$

where F is the force applied to the upper plate in Newtons, A is the area of the plate in m^2 and τ is the shear stress in Pa. This force is also characterized by the shear rate which is the fluid flow rate with respect to the distance between two plates. It is given by:

$$\dot{\gamma} = \frac{v}{d} \tag{14}$$

where, v is the velocity of the upper plate, d is the distance between the two plates and $\dot{\gamma}$ is the shear rate. Using these two parameters, viscosity η can be determined by the relation:

$$\eta = \left(\frac{\tau}{\dot{\gamma}}\right)^n \tag{15}$$

where, n is the power law exponent known as the rheological index which determines whether the fluid is Newtonian or non-Newtonian. A Newtonian fluid follows Newton's law and the viscosity does not vary with the varying shear rate, thus, the value of $n = 1$. Fluids in which the viscosity varies with the shear rate are known as Non-Newtonian. These non-Newtonian fluids are further classified as shear thinning (dilatant fluids) and shear thickening (pseudo-plastic) fluids when the value of $n > 1$ and $n < 1$, respectively.

This viscosity denoted by η is known as shear viscosity or dynamic viscosity. Introducing a gravitational effect in the shear viscosity gives ν which is the kinematic viscosity. The effect of gravity is introduced using the density of the fluid ρ and is given by the equation:

$$\nu = \frac{\eta}{\rho} \tag{16}$$

The units of kinematic viscosity are m/s^2 and both η and ρ should be computed at the same ambient conditions, *i.e.*, the same temperature and pressure.

In this work, we will focus on calculation of the shear viscosity of liquids and we will refer to it as viscosity unless specified otherwise.

Using Molecular Dynamics, a deeper insight can be gained in the material's behavior, its molecular structure and composition. Given the feats of MD and its development throughout the years, viscosity calculation still poses a continuous challenge to scientists and researchers even though several methods have been developed to compute it.

The methods to calculate viscosity using MD simulations can be grouped into two categories based on the underlying mechanism – the equilibrium Molecular Dynamics (EMD) and the non-equilibrium molecular dynamics (NEMD). The equilibrium methods are based on fluctuations of pressure and/or momentum. The non-equilibrium methods utilize steady shear using either a periodic shear flow or sliding boundary conditions which will be discussed in more detail in the subsequent sections [52]. Both of these methods are based on time-reversible equations of motion.

2.2.2. Non-Equilibrium molecular dynamics

A system is said to be in a non-equilibrium state when it deviates from its equilibrium state (characterized by constant values of the defining parameters of the system) due to external perturbations. A response theory is needed to analyze the behavior of a perturbed non-equilibrium system for which no complete theory exists. This is achieved in Molecular Dynamics by replacing the source of perturbation by a series of controls through which several system variables such as temperature, pressure, induced stress, *etc.* can be tuned locally. In this way, a link between microscopic dynamics and macroscopic quantities is achieved for the non-equilibrium state. This link has enabled us to understand the molecular level phenomena by understanding the system constraints which are useful for computing the macro scale properties of the system.

Typically, MD equations of motions are derived from a Hamiltonian which is simply the total energy of the system for a closed system. In large complex systems, it is convenient to remove unimportant degrees of freedom and replace these DoFs by constraints. The most convenient way to handle these constraints is by using an explicit expression for Lagrange multipliers and modifying the equations of motion. In simulations with applied external forces, the equations of motion must be supplemented with a thermostatting mechanism in order to compensate for the energy input due to external artificial forces such as in the case

of the planar Couette flow. The resulting equations of motion in the phase space $\mathbf{x} = (\mathbf{r}, \mathbf{p}) = (\mathbf{r}_1, \mathbf{r}_2, ..., \mathbf{r}_N, \mathbf{p}_1, \mathbf{p}_2, ..., \mathbf{p}_N)$ are non-Hamiltonian [53]:

$$m_i \ddot{\mathbf{r}}_i = \mathbf{F}_i - \lambda_\alpha(\mathbf{x}) \nabla_i \sigma(\mathbf{r}) \tag{17}$$

where $\mathbf{F}_i = -\nabla_i V$ is the force on particle i due to the potential energy V and $\sigma(\mathbf{r}) = 0$ is the holonomic constraint to which the system is subjected. This constraint could be a bond constraint or a reaction coordinate constraint imposed in the simulation. The second term in Eq. (17) describes the constraint forces with Lagrange multipliers. $\lambda_\alpha(\mathbf{x})$ are the Lagrange multipliers with the explicit expression [54]:

$$\lambda_\alpha(\mathbf{x}) = \frac{\left(\sum_i \frac{\mathbf{F}_i}{m_i} \cdot \nabla_i \sigma + \sum_{i,j} \frac{\mathbf{p}_i}{m_i} \cdot \frac{\mathbf{p}_j}{m_j} : \nabla_i \nabla_j \sigma \right)}{\sum_i \frac{1}{m_i} (\nabla_i \sigma)^2} \tag{18}$$

The average of the desired dynamical quantity $\bar{A}(t)$ is obtained using the evolution operator $U(t, t_0)$ for a system evolving from time t_0 to t under fully perturbed dynamics by taking the phase space average over the arbitrary initial system represented by ρ_0 as follows:

$$\bar{A}(t) = \int \mathbf{dx} (U(t, t_0) A(\mathbf{x}) \rho_0(\mathbf{x}))$$

One of the drawbacks of the NEMD methods is the huge strength of perturbation required at the macroscopic scale to be able to produce a detectable response (greater than the statistical noise) at the microscopic level. At such large perturbation strengths, one cannot be sure whether the linear or non-linear regime of perturbations is investigated. This issue can be solved by using the *subtraction technique* which allows decreasing the noise of the response, thereby eliminating the need for greater perturbation strength. In this technique, two different trajectories are obtained - perturbed and unperturbed, their difference is obtained and averaged over all segments of the run. The dynamical variables thus computed with and without the subtraction technique have same dynamical response but significantly different variance.

The MD simulations in this work were carried out using the Large-scale Atomic/Molecular Massively Parallel Simulator (LAMMPS) [33]. The implementation of LAMMPS has four NEMD methods for calculation of viscosity:

1. Induce the flow gradient or the momentum flux and monitor the quantities of interest
2. The wall is dragged over the fluid to induce shear
3. NEMD shear deformation with SLLOD
4. Müller-Plathe reverse perturbation method

2.2.3. SLLOD method

One of the most popular methods for viscosity calculation in non-equilibrium molecular dynamics is the SLLOD method or the SLLOD perturbation which essentially is a way to computationally impose a Couette flow. A Couette

flow in fluid dynamics is a viscous fluid flow between two surfaces where one moves tangential to the other. Physically, this kind of flow is evident between two parallel plates or between two concentric cylinders. This flow is used for viscosity computation in MD because of the similarity with experiment where shear is applied to the top boundary in order to develop a linear velocity profile. This velocity profile is correlated with viscosity according to the following equation:

$$\eta = -\frac{p_{xy}}{\dot{\gamma}} \tag{19}$$

where:

$$\dot{\gamma} = \frac{\partial v_x}{\partial y}$$

and p_{xy} is the off diagonal term of the pressure tensor, $\partial v_x/\partial y$ is the transverse velocity gradient also known as shear rate or strain rate and η is the shear viscosity.

The non-Hamiltonian SLLOD equations of motion proposed by Evans and Morriss [35] are:

$$\dot{\mathbf{r}}_i = \frac{\mathbf{p}_i}{m_i} + \mathbf{r}_i \cdot \nabla \mathbf{v}$$

In this method, the flow induced by SLLOD equations is not generated by the boundaries of simulation box. Correct velocity gradient is obtained as a feature of equations of motions and momentum conservation [18]. These equations of motion must be used in conjunction with suitable PBCs to prevent any interference due to the boundaries. The Lees-Edwards boundary condition is recommended for planar Couette flow and guarantees correct velocity gradient generation in low Reynold's number. This method not only succeeds in transforming a completely boundary driven flow into a flow driven by artificial external field but also generates accurate non-linear response for adiabatic shear flow. SLLOD equations are also compatible with nonlinear response theory and allows drawing of transport properties under weak perturbation strengths.

Along with advantages, there are a few drawbacks of the SLLOD method. The viscosity from this method may not necessarily correspond to the viscosity obtained from experiments. It is not a problem with simple fluids but may give rise to different viscosities for complex ones. This problem is due to the fact that in SLLOD algorithm, instead of a force profile, a linear velocity profile is imposed up to the atomic level. However, in experiments, the external forces that impose a Couette flow act at a macroscopic level. Another shortcoming of this method is the overall rotation it produces in the system [24].

2.3. Lubricant

Propylene Glycol (PG), also known as Propane-1,2-diol is an organic solvent with the chemical formula $C_3H_8O_2$. The selection of this lubricant is simply based on the fact that it is a simple enough structure to model and simulate. Moreover, it is being used as a novel lubricant for combustion engines with CNT additives to be able to reduce friction in such machinery [1]. It has already been used in several studies and is in fact being used in industry as a fuel additive due to its

low viscosity suitable for engine use. It can be regarded as a carrier oil or fluidizer which is added in fuels due to its high thermal stability which prevents fuel deposit formation at very low temperatures. Another advantage of Propylene Glycol is its compatibility with both fuels as well as other lubricants. PG is also used as an antifreeze in Aviation Turbine Fuel (AVTUR) which reduces the freezing point of any accidental water content present in the fuel preventing formation of ice crystals at low temperatures and provides protection against microbial growth. Apart from aforementioned uses of PG, it is also used in E-cigarettes and movie making to create dense smoke.

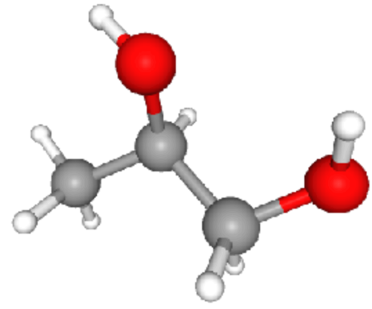

Figure 2. 3D structure of a molecule of Propylene Glycol. In this illustration, grey, red and white spheres denote C, O and H atoms, respectively

In this work, we are concerned with the use of PG as a lubricant in engines and its rheological properties. These properties (measured experimentally) are summarized in the table below.

Table 1. Relevant physical properties of Propylene Glycol at T = 300 K and p = 1 bar

Property	**Value**	**Units**
Density	1.032	g/cm^2
Viscosity	0.042	Pa·s
Thermal Conductivity	0.206	W/(m·K)
Molar mass	76.09	g/mol

3. Methodology

This work focused on the development (and validation) of the methodology for calculating viscosity of liquid lubricants (with additives) using MD. A parallel MD program known as LAMMPS was used for this work [33, 55]. The interatomic interactions were described using a reactive potential called ReaxFF [56].

A method for generating initial structures of the simulated liquid systems (pure PG and PG with CNT additives) was developed and implemented in the form of a C++ computer program. The generated initial structures were equilibrated and later subjected to NEMD simulations. The simulation box was

a tri-clinic cell with periodic boundary conditions in all three directions. Couette flow was simulated by applying uniform shear velocity in x direction to the xy plane to obtain viscosity of the liquid.

The procedure was repeated with different initial conditions to obtain several trajectories. This was done to investigate the sensitivity of results to initial condition. A parametric study was performed in order to find approviate values of parameters such as simulation length and order of imposed shear velocity. Once suitable parameters were obtained, the developed methodology was applied to the system (also PG) with CNT additives. This was done in order to study the influence of CNTs on the rheological properties of lubricants such as Propylene Glycol.

3.1. Initial Structure

To create the initial liquid structure of Propylene Glycol molecules, a single PG molecule was created and then replicated within a triclinic simulation box. The initial tilt factors were set to zero and periodic boundaries were applied in all three directions. The locations of center of mass (CoM) of the molecules were obtained randomly from a uniform distribution. To avoid overlapping molecules, the distance between any pair of atoms (belonging to two PG molecules) was set to a minimum of 2 Å. The orientation of the molecules was also randomly chosen from a uniform distribution. Size of the box was calculated on the basis of required density and amount of molecules in the system. The density of the initial system was kept half of the experimental density of a PG system at room temperature and pressure. The system was densified later during equilibration. The initial structure of system with PG molecules only is shown in Figure 3 and the chosen parameters are given in Table 2.

A similar approach was adopted to create initial structure of lubricant oil with CNT additives with a specified weight percentage. In order to create such a system, CNT molecules were first created by folding a graphene sheet according to diameter and length specifications of the single walled CNTs as shown in Figure 4. Once desired CNT molecule was generated, it was then added to the pure PG system according to a suitable molecular concentration for calculations and with the same minimum distance between any pair of atoms (belonging to two molecules) as 2 Å. The structure thus created is shown in Figure 5.

The parameters of the structures (both cases: pure PG, PG with CNT additives) created and used in the simulations are summarized in Table 2.

This creation of initial structure was done by writing two C++ programs - one for generating Carbon Nanotubes and the other for generating a system with PG and CNT fulfilling aforementioned conditions. The programs create files in *.xyz* format and are converted to LAMMPS data format [57]. The simulations were carried out using the C++ parallel code for Molecular Dynamics LAMMPS [33, 55]. The unit system was chosen to be *real* to suit the requirements related to the usage of reax/c package (LAMMPS implementation of the ReaxFF force field).

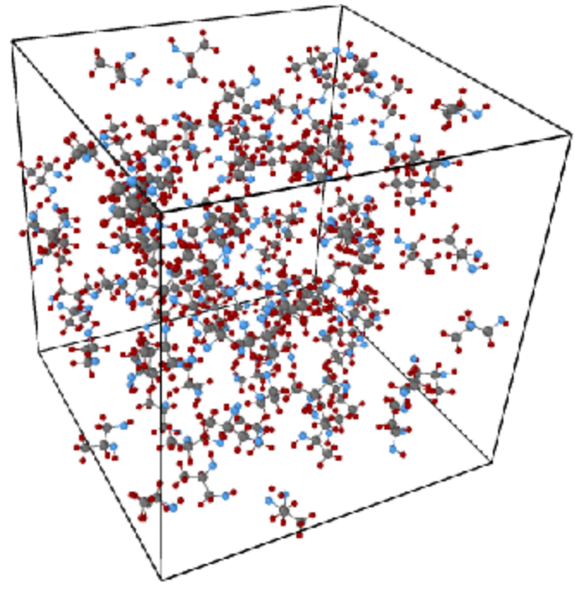

Figure 3. Visualisation of pure system with 100 PG molecules in OVITO with particles unwrapped at periodic boundaries

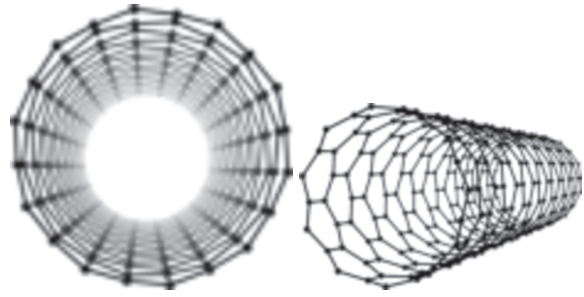

Figure 4. Visualisation of 3D structure of CNT molecule created to be used as additive in the PG system

3.2. High Performance Computing

Molecular Dynamics simulations have an obvious limitation of time scales and size of the system. In this particular problem, the simulations ran too long on a personal computer to be able to gather any useful results. To resolve this issue, simulations were carried out with the use of the Tryton cluster [58], located in the Information Center of the Tri-City Academic Computer Network (CI TASK) [59]. Small test simulations were conducted to obtain the optimum number of nodes required for this work. A system of 100 PG molecules (after equilibration) was simulated for 20,000 steps (further equilibration + viscosity calculation) with different number of MPI processes and the following graph was obtained with this study.

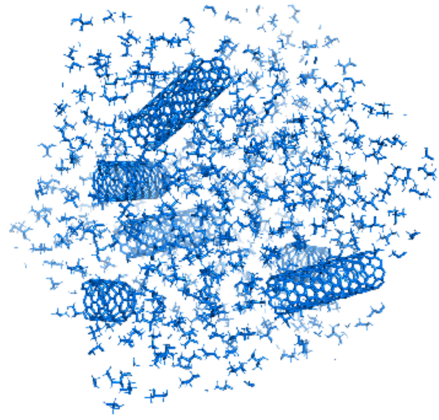

Figure 5. Visualisation of PG system with CNT molecules in PyMOL with particles unwrapped at periodic boundaries

Table 2. Parameters of the structures of both pure PG and PG with CNT additives created and used in the simulations

Parameters	Pure system	Impure system	Units
Simulation box side	30	60	Å
Number density	0.004	0.004	molecules/Å^3
Experimental density	1.032	unknown	g/cm^3
Total molecules	100	510	molecules
Diameter, length of CNT	-	7.82, 24	Å
CNT molecules	-	5	molecules
CNT,PG atoms	- , 1300	1200, 6565	atoms
Total mass of PG atoms	1.263×10^{-20}	6.378×10^{-20}	g
Total mass of CNT atoms	-	2.39×10^{-20}	g
Weight percentage of CNT	-	27	%
Atomic concentration of CNT	-	15.45	%
Molecular concentration of CNT	-	0.98	%

This graph shows the wall time required for a simulation with different number of MPI processes used. A non-linearly decreasing trend is observed in wall-time with $2n$ processes where, n is the number of Tryton cluster nodes; each process using 12 threads. A total of 12 MPI processes were thought to be optimal for our calculations as a significant reduction in wall time was obtained. The wall time reduced further with increasing number of processors but the wait time increased for more processors. This increased wait time did not give a considerable reduction in wall time of the program hence 6 nodes, 12 processes (12 threads per process) were used for all simulations for pure PG.

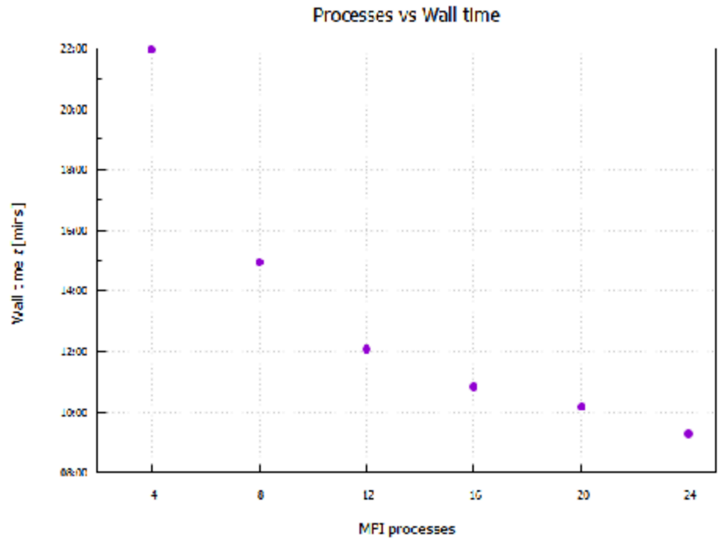

Figure 6. Wall time vs MPI processes for simulation of 100 molecule system for 20,000 steps

The system with CNT additives was much larger and computationally more demanding. A total of 144 and 480 MPI processes were utilised for equilibration and production runs respectively.

3.3. Equilibration

Once the initial structure was created, the next task was to equilibrate the system and densify it so it resembles the system that exists in reality. This was done by controlling the temperature and pressure using an NPT ensemble using a constantly deformed triclinic cell and periodic boundary conditions in all directions. The initial temperature was set to 600 K and pressure to 0 atm along with the target temperature as 300 K and pressure as 1 atm with a damping constant of 100 fs. The motivation behind this choice was for the system to have higher thermal energy in the beginning so it equilibrates faster. Moreover, the pressure was increased for the system to densify itself. Having position of atoms from the generated initial structure (as described in the previous section), velocities were generated for the initial temperature using Gaussian distribution with a given random seed.

The initial charges were set to zero on all atoms. Equilibration input files were created both with and without charge equilibration for comparison but due to computational limitations, only a no charge equilibration model was used.

The pair coefficients used (parameters of the adopted ReaxFF potential) were obtained from the example simulation provided with the LAMMPS. These parameters correspond to the parameterization of the ReaxFF force field developed by Chenoweth *et al.* [37].

The time step of the simulation was set to 0.1 femtoseconds. The simulation was run for few hundred thousand femtoseconds until thermodynamic quantities such as temperature, pressure, density and energy of the system became constant. 10 independent simulations were run, each was started with different seed used in the random generation of the initial velocities. Once equilibrated systems were obtained, they were used (as initial structures) for production runs to compute viscosity using the SLLOD method.

The time evolution of the thermodynamic parameters (temperature, total energy, density) in the equilibration is presented in Figures 7 and 8. Equilibration of a system can be confirmed by simply monitoring these parameters during the course of the equilibration run. In these figures, average value of those parameters are presented for every 300 thousand time-steps. It is seen that the parameters become constant after some time, *i.e.*, they fluctuate around well-defined value. Physically, this means that the state of the system does not change.

Figure 7 shows the temporal evolution of parameters for pure PG system and Figure 8 for the system with CNT additives. We observe that for each system it takes different time to reach equilibrium state. This is because each system evolves with different trajectories. It is seen that the value of density stops fluctuating after a very long time while total energy and temperature are quick to equilibrate.

The density for pure system converges to value 1.06 g/cm^3 which is close to the experimental value 1.04 g/cm^3 with an error of 1.9%. It can be seen from Figure 7 that some seeds take longer than others to equilibrate to the desired value of density.

The density of PG system with CNT additives was not known *a priori* but was found (from the carried out simulations) to converge to a value of 1.26 g/cm^3 at 300 K temperature with pressure of 1 atm. It takes significantly longer to equilibrate the system containing CNT additives.

3.4. Production run

The production runs were conducted using the NVT/SLLOD ensemble with the ReaxFF potential using the data file generated as a result of equilibration runs. This data file contains position, velocities and charges on each atom. The temperature was set to 300 K and controlled by Berendsen thermostat. Again, the charge equilibration was switched off. The system was subjected to shear by using the Lees-Edwards boundary conditions, *i.e.*, by imposing a velocity in x direction on the top edge of the simulation box. After imposing this velocity, the system was further equilibrated before recording shear stress and velocity profile data. Temperatures that were computed by LAMMPS during this simulation were distorted due to the tilt of the box which generates a bias velocity. This bias velocity was subtracted from velocities of all atoms in the system to give thermal velocity which was then used to compute true temperature. The velocity profile was obtained by dividing the simulation box into bins in the y direction

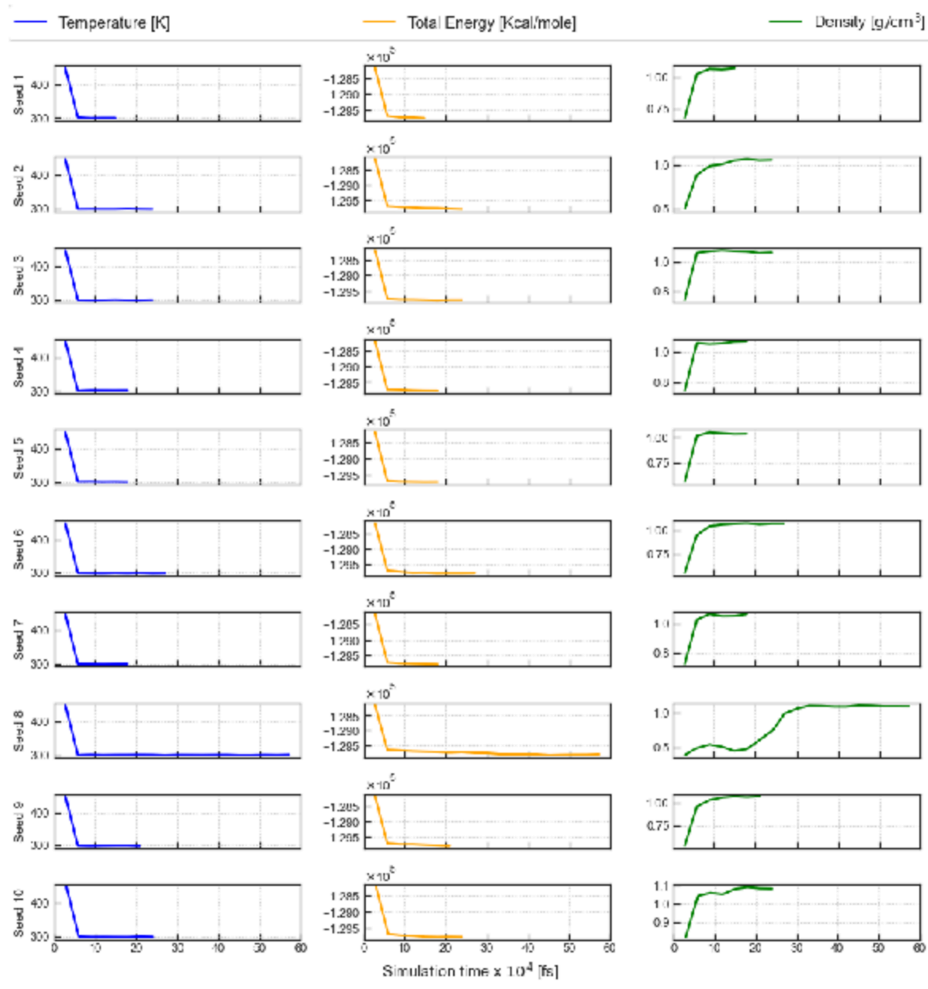

Figure 7. Evolution of thermodynamic parameters (temperature, total energy, density) for pure PG system during equilibration

(each containing at least a few hundred atoms) and time-averaging the velocities of atoms belonging to particular bins.

Viscosity calculations (actual production run) were done after this equilibration by running the system for another few hundred thousand steps. During this stage the instantaneous and time averaged values of calculated viscosity were recorded.

4. Results

4.1. Pure system - PG molecules only

The results of the simulation for system with only Propylene Glycol molecules are presented and discussed in this section.

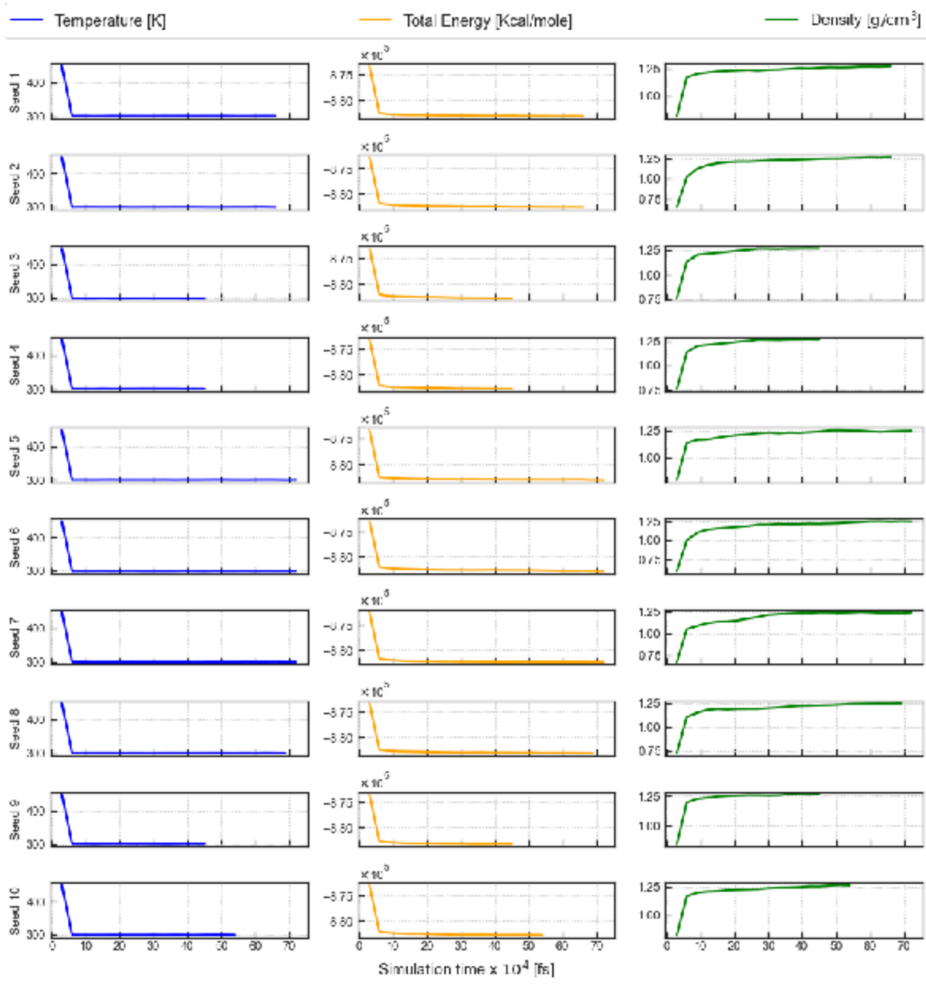

Figure 8. Evolution of thermodynamic parameters (temperature, total energy, density) for system with CNT additives during equilibration

4.1.1. Influence of imposed shear

An important aspect of this simulation is the applied shear which influences the viscosity calculation. To obtain the optimum value of shear, several shear rates were imposed by specifying shear velocity to find the optimum value of shear rate. The results from these simulations are presented in Figure 9.

It is observed that the viscosity for lower shear velocities is negative and quite far from experimental value. A negative viscosity would mean that the fluid is being propelled beyond the imposed shear which is possible in bacterial suspension fluids [60]. A truly negative viscosity is also achieved in magnetic nano-fluids subjected to alternating magnetic fields [61]. However, in our case, the fluid is a simple lubricant which exhibits positive viscosity at normal temperature

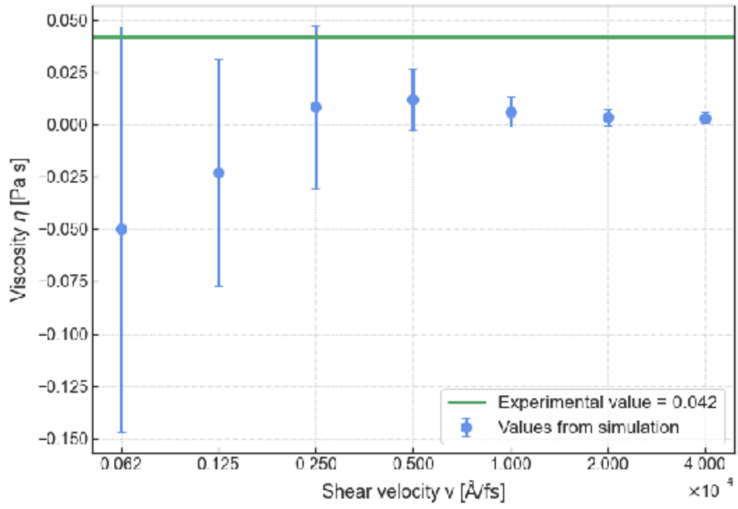

Figure 9. Log plot of viscosity vs shear velocity for pure system after 10^5 time-steps

and pressure. Therefore, it could be an artefact of system not being in equilibrium state thereby adding energy to the system. This result raises another important question for viscosity calculation using SLLOD method - is the simulation time of 10^5 steps with a time step size of 0.1 fs enough? This question is answered in the next subsection.

4.1.2. Influence of simulation time

To check the effect of simulation time and obtain the optimum simulation length, a parametric study was performed for 3 shear velocities and the results are summarized in the following plots.

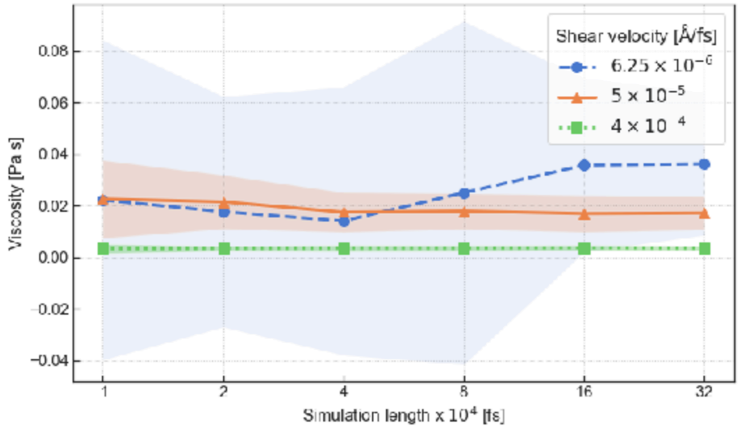

Figure 10. Evolution of instantaneous viscosity averaged over 10 trajectories with simulation time on a log plot. The shaded regions indicate standard deviation from the mean value

From Figure 10, it can be observed that the viscosity has not converged to a final value even after 3.2 million time-steps. For shear velocity 4×10^{-4} Å/fs, the viscosity seems convergent but the viscosity obtained is by one order less than the experimental value. Therefore, we can discard this observation completely. For lower shear velocities, the viscosity value is of the correct order - experimental value being 0.042 Pa·s. Viscosity for lowest shear velocity 6.5×10^{-6} Å/fs has closer value to experimental one but converges very slowly and requires a much longer simulation. Viscosity evolution for moderate shear velocity of 5×10^{-5} Å/fs looks convergent but would require a longer simulation to confirm. Since computational resources are limited for the scope of this work, we assume that the shear velocity of 5×10^{-5} Å/fs gives reasonable results for a simulation time of 3.2 million time-steps.

Figure 11 shows the running average of viscosity and confirms that for the limited simulation time, shear velocity of 5×10^{-5} Å/fs exhibits an almost convergent behaviour.

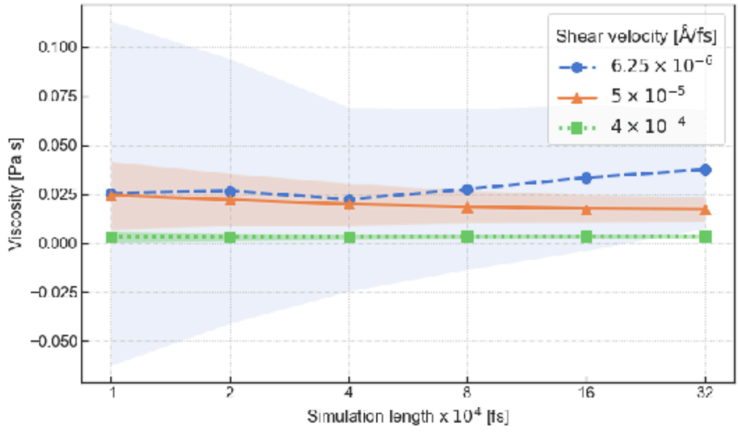

Figure 11. Running average of viscosity over 10 trajectories vs simulation time. The shaded regions indicate standard deviation from the mean value

In order to understand this behaviour of the system, we look at the evolution of total energy of the system after the application of shearing force (see Figure 12). It is clear from the graph that the three systems with different shear rates all reach a different energy configuration at the end of 3.2 million time-steps. This explains the difference in computed viscosity. Moreover, the differences in the energy of the system are quite significant for the two extreme values of shear velocities. This confirms that the simulation time of 3.2 million time-steps is not enough for precise viscosity computation using current methodology.

A deeper insight in this problem can be gained by analysing velocity profiles with increasing simulation time for various shear velocities as shown in Figure 13. The symmetry in velocities between upper and lower half of the simulation box is marked with shading them yellow and green, respectively. For clarity of results,

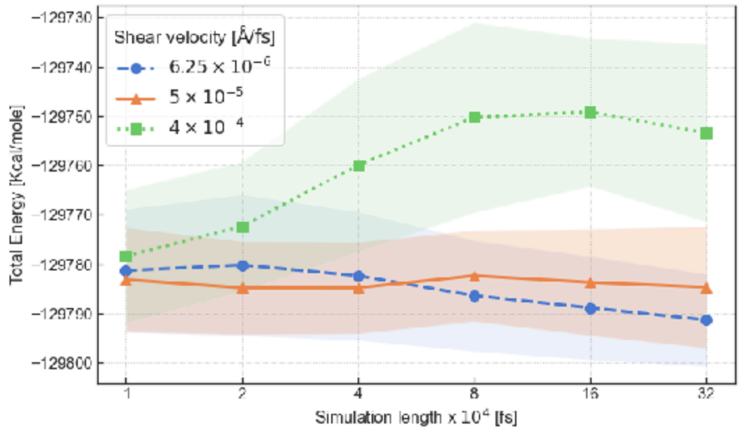

Figure 12. Evolution of total energy with simulation time for pure PG system on a log plot. The shaded regions indicate standard deviation from the mean value

the color is also used to distinguish velocity profiles corresponding to different simulation times. Greater the simulation time, darker is the color of the profile in the plot.

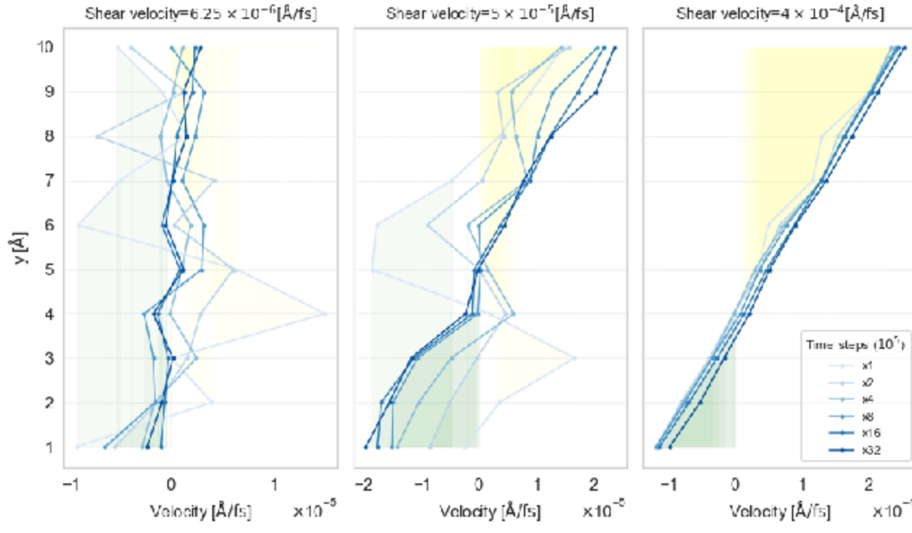

Figure 13. Temporal development of velocity profiles for three cases of shear imposed on a pure PG system. The shaded regions show asymmetry of the velocity profile

From the nature of NEMD simulation methodology where a planar Couette flow is imposed, a linear velocity profile is expected from the exact solution of continuum problem. The linearity is confirmed in this graph for all the shear velocities. However, a lot of noise is observed for smaller simulation lengths which means that the flow has not reached steady state for accurate calculations of viscosity.

This explains the high uncertainty in computed viscosity seen in Figure 9 for 10^5 steps. With the increase in simulation time, linear behaviour can be clearly observed as the initial transients have decayed and a steady flow is obtained.

For very low value of imposed shear, the velocity profile evolves at a rather slow pace and is extremely noisy. On the other hand, for very high shear, the velocity is always linear, it evolves very quickly to achieve steady flow but the asymmetry is clearly visible. The asymmetry is an indicator of poor momentum transfer along the y direction.

4.1.3. Dependence of viscosity on imposed shear velocity

The noise from the velocity profiles observed in the previous section can be eliminated by fitting the data with the linear function. The slope gives the velocity gradient $\partial v_x/\partial y$ and the intercept gives the asymmetry of momentum transfer between top and bottom boundaries of the simulation box. The values of x component of velocity are taken after 3.2 million time-steps for the three cases of imposed shear. From these values, viscosity can be obtained by using Eq. (19).

Figures 14, 15, 16 show the fit, corresponding values of velocity gradient, asymmetry constant as well as the viscosity obtained using Eq. (19) for imposed shear of the order of 10^{-6}, 10^{-5} and 10^{-4} Å/fs respectively. The viscosity obtained from this method for all shear rates are summarized in Figure 17.

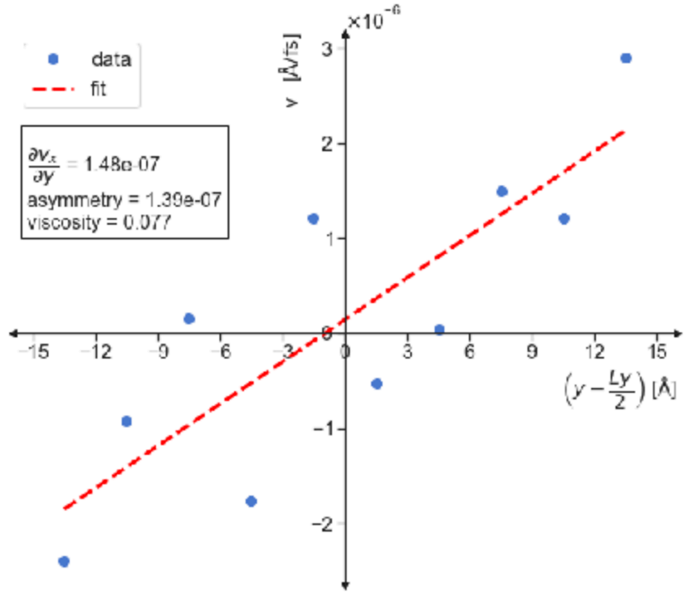

Figure 14. Linear curve fitting of the velocity profile for pure system after 3.2 million time-steps of imposing a shear velocity of 6.5×10^{-6} Å/fs

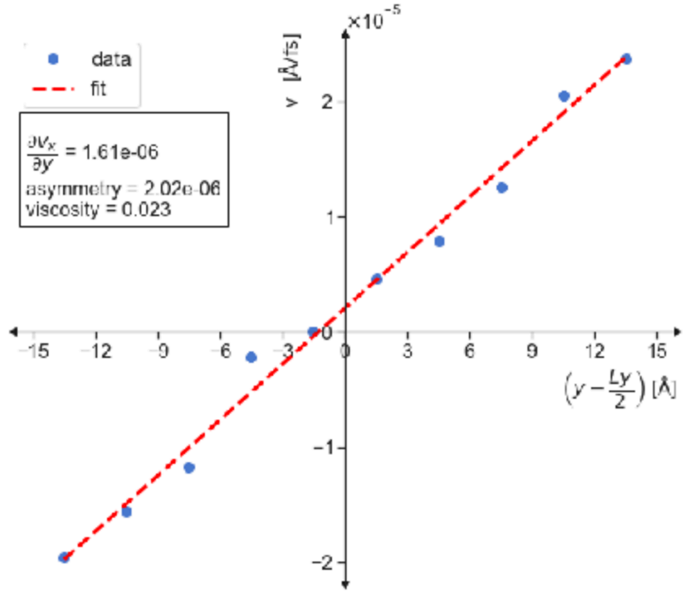

Figure 15. Linear curve fitting of the velocity profile for pure system after 3.2 million time-steps of imposing a shear velocity of 5×10^{-5} Å/fs

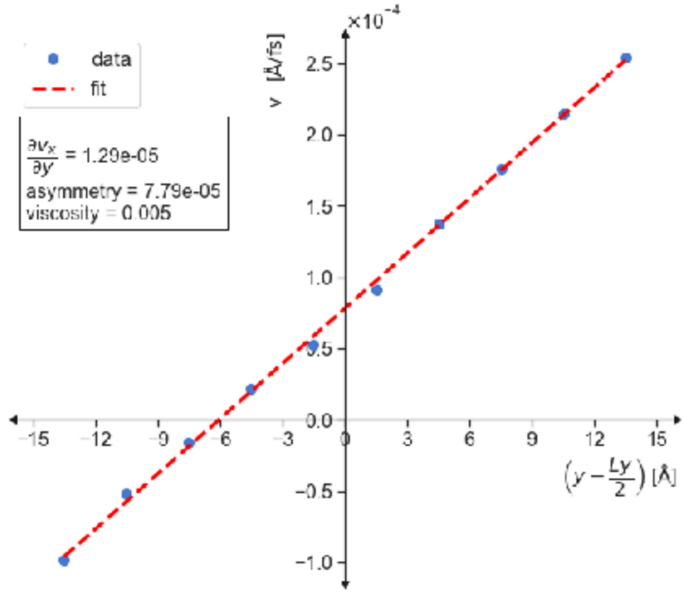

Figure 16. Linear curve fitting of the velocity profile for pure system after 3.2 million time-steps of imposing a shear velocity of 4×10^{-4} Å/fs

Figure 17 presents the effect of shear rate on the viscocity of the pure lubricant system using ReaxFF potential and NEMD viscosity calculation method. It

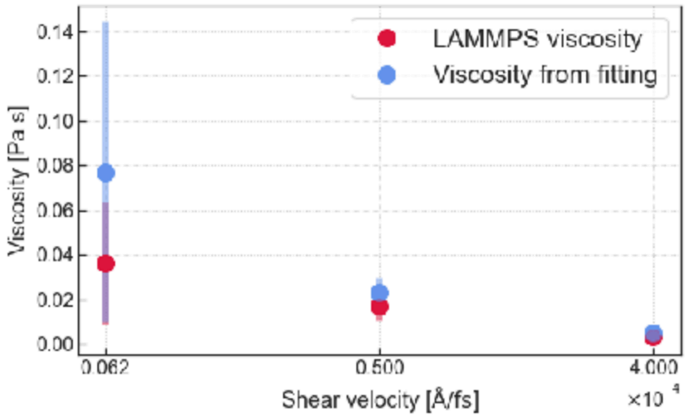

Figure 17. Viscosity for various shear velocities for pure PG system

is observed that the viscosity shows a clear decreasing trend with increasing shear rate. This shear thinning behaviour of lubricants subjected to high imposed shear has been described as a consequence of NEMD methods for rheological computations of liquid lubricants [11]. For high values of imposed shear, Newtonian liquid lubricants exhibit a Non-Newtonian behaviour. This can be avoided by applying smaller values of imposed shear in which case, a Newtonian plateau is obtained (shear rate does not influence viscosity). However, for smaller values of imposed shear, a very long simulation time might be necessary for the system to reach an equilibrium state - even with the best of computational resources. The lowest value of shear velocity studied for this work was of the order of 10^{-6}. The total wall time for a single simulation with only pure PG molecules using 48 MPI processes was 34 hours (1.4 days). This system consisted of only 100 molecules. On the other hand, the system with CNT additives was composed of 510 molecules and was more demanding. The total wall time for one such simulation was approximately 260 hours (11 days). 140 MPI processes were used for equilibration runs and 480 MPI processes for production runs on the Tryton cluster. This was clearly not sufficient to obtain a good value of viscosity as is evident from Figure 17. Hence, even longer simulation time might be required to accurately compute steady state viscosity of the system of liquid lubricants at lower shear rates and obtain the Newtonian plateau.

Another important result of this study is seen in Figure 17 which is the difference of viscosity values obtained by various methods of averaging and calculation. This is due to the fact that NEMD methods are known to be highly sensitive to averaging techniques which is a factor that should be considered while setting up the LAMMPS simulation as well as during post-processing. The values might vary depending on the method used for calculation.

As far as the choice for imposed shear is considered given the currently available computational resources as well as the scope of this work, the value

of 5×10^{-5} Å/fs is a good compromise as the value of viscosity is closer to the experimental one, albeit with a significant error of around 43%.

4.2. Influence of CNT additives in Propylene Glycol

Having selected suitable parameters for rheological calculation using a reactive force field and an NEMD approach, the simulations are performed with CNT immersed in liquid lubricant Propylene Glycol. CNT additives are expected to enhance the viscosity of the lubricant thus enhancing the anti-friction properties of the lubricant. Since the system with CNTs is more complex than pure lubricant, a lot of computational challenges are also expected. As we have already seen that a much longer simulation time is required for equilibration of this system, the same is expected for the production runs.

Couette flow with a shear velocity of 5×10^{-5} Å/fs is imposed on a 60 $Å^3$ triclinic cell containing 5 CNTs and 505 PG molecules. The system is run for 3.2 million time-steps with the same time-step size of 0.1 fs so as to reach steady state before calculation of viscosity.

4.2.1. Velocity Profile

The velocity profile is studied for the new system with CNT additives to check whether the flow after 3.2 million time-steps is linear. The system is divided into 62 bins along y axis to compute velocity average for each slab containing >100 atoms.

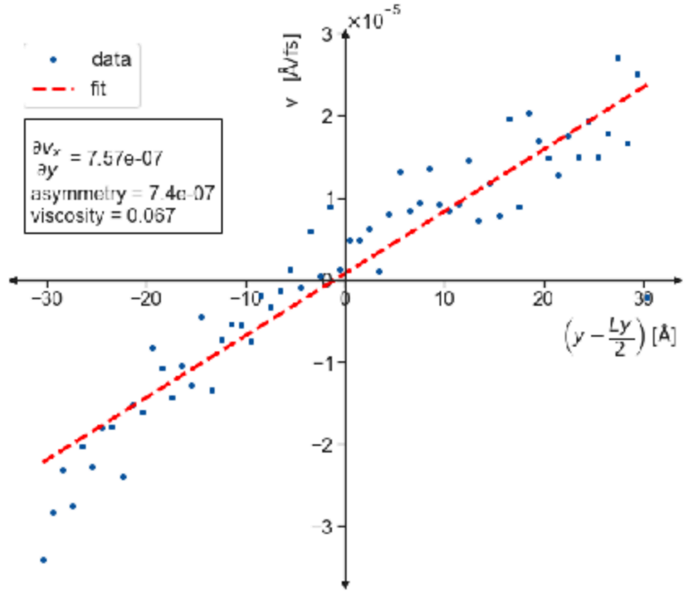

Figure 18. Velocity profile for lubricant system with CNT additives

In Figure 18, it is observed that the velocity profile is linear and symmetric between the top-half and the bottom-half of the simulation box. The momentum

transfer across the fluid is much better than in the case of no CNT added to the lubricant. The slope or the velocity gradient in y direction is also much lower (1.61×10^{-6} fs^{-1}) than in the previous case (7.57×10^{-7} fs^{-1}). Few outliers are seen in the velocity data from LAMMPS at the extreme edges of the simulation box. This could be due to <50 atoms in the first and the last slab for velocity averaging which leads to poor averaging in those bins.

4.2.2. Dispersion of CNT in the lubricant

CNTs typically show a strong tendency to agglomerate due to their large surface area [1]. This is an important property to study because the agglomerates degrade the tribological properties of the lubricating engine oils. It could even have severe consequences if the agglomerates block the engine oil filter in internal combustion engines. Certainly, this is not the case for all oils with CNT additives. The agglomeration greatly depends on the size, type (single-walled or multi-walled) and concentration of CNTs in the lubricant. This study however, is limited to only a single case of all aforementioned parameters. Figures 19 and 20 show the spatial distribution of CNTs before and after the imposed shear respectively. These figures provide no evidence of severe agglomeration of CNTs which could be attributed to the small length of CNT used for this simulation. However, some CNTs tend to move in a small space which could be just the effect of densification of the system. Needless to say, this study demands more research than in the scope of this work.

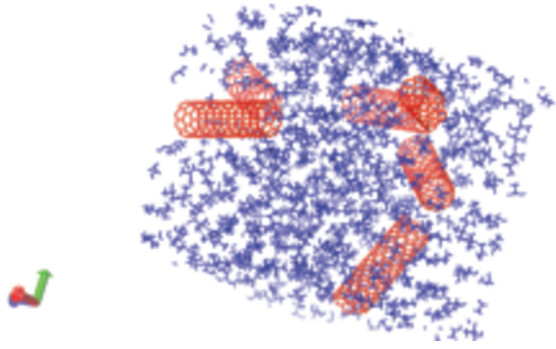

Figure 19. Distribution of CNT and PG molecules before the simulation

4.2.3. Viscosity

The influence on rheological properties of the liquid lubricants upon dispersion of CNTs can be clearly seen from Figure 21. An increase of 100-190% (depending on the method used for calculating viscosity) in viscosity value is observed with an addition of 27 wt% of CNTs to the lubricant. CNTs provide additional resistance to flow which slows the momentum transfer in the direction perpendicular to the flow. This clearly shows the potential of CNT additives for enhancing anti-friction properties of the lubricant especially in hydrodynamic regimes.

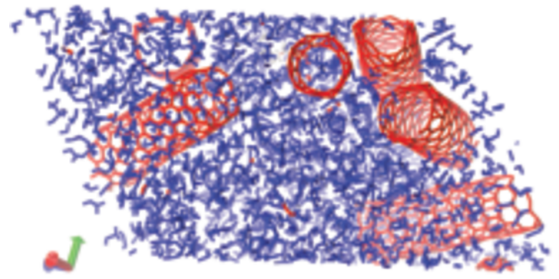

Figure 20. Distribution of CNT and PG molecules after the simulation

Although the results seem promising, a careful look at the error margin of these calculations reveals that for the system with CNTs, the error is significant. Moreover, the experimental value of such a system is unknown so a fair validation of the methodology employed for this work may not be possible yet. However, a qualitative analysis of the lubricant's rheological properties can be done to understand the system at a molecular level. We see yet again that different averaging techniques yield different results which is due to the NEMD method used. The viscosity obtained from various methods for both the systems is summarized in Table 3.

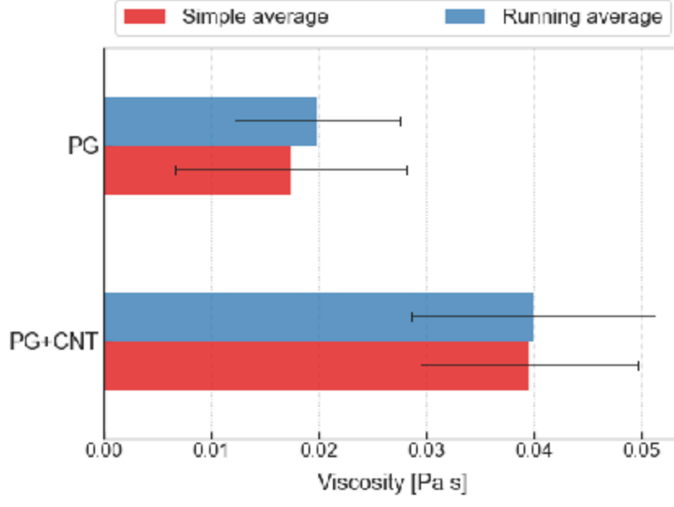

Figure 21. Influence of CNT addition in Propylene Glycol on viscosity of the system

5. Conclusion

This research project aimed to study the influence of addition of CNT to the lubricant such as Propylene Glycol on its rheological properties by performing NEMD-SLLOD simulations using LAMMPS with inter-atomic forces described using a reactive force field ReaxFF. C++ programs were written to generate

Table 3. Comparison of viscosity values (in Pa·s) for pure lubricant and lubricant with CNT additives calculated using various averaging techniques

Viscosity calculation method	PG	PG+CNT	Percentage increase
Simple averaging	0.0174	0.0395	127%
Running average	0.0198	0.0399	100%
Fitting from velocity profile	0.023	0.066	186%
Average of above three methods	0.02	0.048	140%

periodic triclininc initial structures for LAMMPS and they were subject to equilibration and allowed to evolve in 10 different trajectories using varying seeds for initial velocity. A parametric study was performed for developing the methodology for simulating organic lubricants. Based on the parametric study, it was concluded that the simulation time of 3.2 million time-steps with a 0.1 fs time-step size was not sufficient for the lubricant system to reach equilibrium state and thus a reliable calculation of viscosity cannot be made. Moreover, an imposed shear velocity of the order of 10^{-5} Å/fs is suitable for the given configuration of system as well as computational resources. Non-Newtonian behaviour of a Newtonian fluid was observed as a result of NEMD method used. After obtaining suitable parameters, the error in computed viscosity was obtained to be approximately 43% from the experimental value for a pure system with only PG molecules.

Moving towards the system with CNT additives, the viscosity of PG with CNT additives was obtained to be 0.048 Pa·s compared to 0.02 Pa·s of pure PG. This corresponds to a 100-190% increase in the viscosity of PG by addition of 27 wt% of CNTs. Although this result answers the main research question of this project, it comes with a high uncertainty in computed viscosity due to computational errors and limited computational resources. Therefore, this report gives a more qualitative view on the influence of rheological properties upon addition of CNT to organic lubricants.

5.1. Problems encountered during research

Several difficulties were faced to obtain optimum parameters and validate the methodology for rheological calculations of lubricants using NEMD. Some of these are discussed below:

1. The time-scale obtained using state-of-the-art computational facilities was insufficient to capture the steady state value of viscosity.
2. Shear thinning of Newtonian fluid begs obtaining the optimum value of imposed shear for accurate viscosity calculations. A Newtonian plateau must be obtained where the viscosity is independent of imposed shear. This was impossible with the available computational resources.
3. Variation in the value of viscosity was obtained using different averaging methods which shows extreme sensitivity of NEMD simulations to averaging techniques.

4. Few simulations ended unsuccessfully which may be due to several reasons such as unphysical behaviour of the system, memory leaks, unstable algorithms *etc.* This remains undetermined due to the scope of the work and needs further discussion.

5.2. Practical implications of viscosity enhancement

Increase in viscosity of a lubricant such as Propylene Glycol means that it will form a thicker layer between surfaces in contact with each other thereby eliminating the friction between them. It will thus enhance anti-friction and anti-wear properties. Since viscosity of the liquid decreases with temperature, a higher viscosity works well at maintaining the anti-friction layer when the surfaces get hotter during operation. Moreover, a viscous liquid spreads more evenly making it desirable for engines with complex design.

5.3. Future Scope

This report was a foundation work for further research on the topic as robust and accurate rheological computations using Molecular Dynamics remains a huge challenge till date. This work motivates a larger scale parametric study with larger systems simulated at much longer time-scales. More independent trajectories and initial structures need to be analysed in order to obtain a value with minimum uncertainty. Shear rate, size of the system, concentration, type and size of additives, simulation time, *etc.* are some parameters that need an in-depth analysis. Other equilibrium and non-equilibrium methods may be studied to be able to make a comparative analysis of ability of accurate viscosity calculations. Apart from the methods, several force-fields could be used to describe atomic interactions within the system and a study of appropriate potential could be done. To summarize, the scope of this research problem is limitless as we still face several challenges in computing rheological properties of liquid lubricants.

References

[1] Kałużny J, Merkisz-Guranowska A, Giersig M and Kempa K 2017 *Lubricating performance of carbon nanotubes in internal combustion engines – engine test results for CNT enriched oil*, *International Journal of Automotive Technology* **18** (6) 1047

[2] Bhaumik S, Prabhu S and Singh K J 2014 *Analysis of tribological behavior of carbon nanotube based industrial mineral gear oil 250 cst viscosity*, *Advances in Tribology* 341365

[3] Alaa M, Osman T A, Khattab A and Zaki M 2015 *Tribological behavior of carbon nanotubes as an additive on lithium grease*, *Journal of tribology* **137** (1) 11801

[4] Gong K, Lou W, Zhao G, Wu X and Wang X 2021 *MoS2 nanoparticles grown on carbon nanomaterials for lubricating oil additives*, *Friction* **9** 747

[5] Rejvani M, Saedodin S, Vahedi S M, Wongwises S and Chamkha A J 2019 *Experimental investigation of hybrid nano-lubricant for rheological and thermal engineering applications*, *Journal of Thermal Analysis and Calorimetry* **138** 1823

[6] Chauveau V, Mazuyer D, Dassenoy F and Cayer-Barrioz J 2012 *In Situ Film-Forming and Friction-Reduction Mechanisms for Carbon-Nanotube Dispersions in Lubrication*, *Tribology letters* **47** (3) 467

[7] Spikes H 2015 *Friction Modifier Additives*, *Tribology letters* **60** (1) 5

[8] Meng Y, Xu J, Jin Z, Prakash B and Hu Y 2020 *A review of recent advances in tribology*, *Friction* **8** (2) 221
[9] Zhao J, Huang Y, He Y and Shi Y 2021 *Nanolubricant additives: A review*, *Friction* **9** 891
[10] Martini A, Eder S J and Dörr N 2020 *Tribochemistry: A review of reactive molecular dynamics simulations*, *Lubricants* **8** (4) 44
[11] Ewen J P, Heyes D M and Dini D 2018 *Advances in nonequilibrium molecular dynamics simulations of lubricants and additives*, *Friction* **6** (4) 1
[12] Ewen J P, Gattinoni C, Thakkar F M, Morgan N, Spikes H A and Dini D 2016 *Nonequilibrium molecular dynamics investigation of the reduction in friction and wear by carbon nanoparticles between iron surfaces*, *Tribology letters* **63** (3) 38
[13] Maginn E J, Messerly R A, Carlson D J, Roe D R and Elliott J R 2019 *Best Practices for Computing Transport Properties 1. Self-Diffusivity and Viscosity from Equilibrium Molecular Dynamics [Article v1.0]*, *Living Journal of Computational Molecular Science* **1** (1) 6324
[14] Posch, H A and Hoover, W G 1992 *Nonequilibrium Molecular Dynamics of Classical Fluids*, *Molecular Liquids: New Perspectives in Physics and Chemistry* 527
[15] Raghavan B V and Ostoja-Starzewski M 2017 *Shear-thinning of molecular fluids in Couette flow*, *Physics of Fluids* **29** (2) 23103
[16] Jabbari F, Rajabpour A and Saedodin S 2017 *Thermal conductivity and viscosity of nanofluids: A review of recent molecular dynamics studies*, *Chemical engineering science* **174** 67
[17] Kaburaki H 2005 *Thermal transport process by the molecular dynamics method*, *Handbook of Materials Modeling*, Springer Netherlands
[18] Todd B D and Daivis P J 2017 *Nonequilibrium Molecular Dynamics*, *Handbook of Materials Modeling*, Cambridge University Press
[19] Hoover W G, Hoover C G and Petravic J 2008 *Simulation of two- and three-dimensional dense-fluid shear flows via nonequilibrium molecular dynamics: comparison of time-and-space-averaged stresses from homogeneous Doll's and Sllod shear algorithms with those from boundary-driven shear*, *Physical Review. E, Statistical, Nonlinear, and Soft Matter Physics* **78** (4) 46701
[20] Calderon C P and Ashurst W T 2002 *Comment on reversing the perturbation in nonequilibrium molecular dynamics: an easy way to calculate the shear viscosity of fluids*, *Physical Review. E, Statistical, Nonlinear, and Soft Matter Physics* **66** (1) 13201
[21] Bordat P and Müller-Plathe F 2002 *The shear viscosity of molecular fluids: A calculation by reverse nonequilibrium molecular dynamics*, *The Journal of Chemical Physics* **116** (8) 3362
[22] Pan G, Ely J F, McCabe C and Isbister D J 2005 *Operator splitting algorithm for isokinetic SLLOD molecular dynamics*, *The Journal of Chemical Physics* **122** (9) 94114
[23] Mundy C J, Siepmann J I and Klein M L 1995 *Decane under shear: A molecular dynamics study using reversible NVT-SLLOD and NPT-SLLOD algorithms*, *The Journal of Chemical Physics* **103** (23) 10192
[24] Hess B 2002 *Determining the shear viscosity of model liquids from molecular dynamics simulations*, *J. Chem. Phys.* **116** (1) 209
[25] Müller-Plathe F 1999 *Reversing the perturbation in nonequilibrium molecular dynamics: an easy way to calculate the shear viscosity of fluids*, *Physical Review E, Statistical physics, plasmas, fluids, and related interdisciplinary topics* **59** (5) 4894
[26] Kałużny J, Kulczycki A, Dzięgielewski W, Piasecki A, Gapiński B, Mendak M, Runka T, Łukawski D, Stepanenko O, Merkisz J and Kempa K 2020 *The Indirect Tribological Role of Carbon Nanotubes Stimulating Zinc Dithiophosphate Anti-Wear Film Formation*, *Nanomaterials (Basel, Switzerland)* **10** (7) 1330

[27] Sekrani G and Poncet S 2018 *Ethylene- and Propylene-Glycol Based Nanofluids: A Litterature Review on Their Thermophysical Properties and Thermal Performances*, *Applied Sciences* **8** (11) 2311
[28] Mary A H, Suganthi K S and Rajan K S 2013 *Mechanistic Investigations of Viscosity and Thermal Conductivity Enhancement in Multi-Walled Carbon Nanotubes-Propylene Glycol Nanofluids*, *Nanoscience and nanotechnology letters* **5** (10) 1125
[29] Kirova E M and Norman G E 2015 *Viscosity calculations at molecular dynamics simulations*, *Journal of Physics: Conference Series* **653** (1) 12106
[30] Zhang Y, Otani A and Maginn E J 2015 *Reliable Viscosity Calculation from Equilibrium Molecular Dynamics Simulations: A Time Decomposition Method*, *Journal of Chemical Theory and Computation* **11** (8) 3537
[31] Fernández G A, Vrabec J and Hasse H 2004 *A molecular simulation study of shear and bulk viscosity and thermal conductivity of simple real fluids*, *Fluid phase equilibria* **221** (1–2) 157
[32] Viscardy S and Gaspard P 2003 *Viscosity in molecular dynamics with periodic boundary conditions*, *Physical Review. E, Statistical, Nonlinear, and Soft Matter Physics* **68** (4) 41204
[33] *LAMMPS*, *https://lammps.sandia.gov*
[34] Hoover, W G and Ashurst W T 1975 *Nonequilibrium Molecular Dynamics*, *Theoretical Chemistry*, Elsevier, **1** 1
[35] Evans D J and Morriss O P 1984 *Non-Newtonian molecular dynamics*, *Computer Physics Reports* **1** (6) 297
[36] van Duin A C T, Dasgupta S, Lorant F and Goddard W A 2001 *ReaxFF: A reactive force field for hydrocarbons*, *The Journal of Physical Chemistry A* **105** (41) 9396
[37] Chenoweth K, van Duin A C T and Goddard W A 2008 *ReaxFF Reactive Force Field for Molecular Dynamics Simulations of Hydrocarbon Oxidation*, *J. Phys. Chem. A* **112** (5) 1040
[38] Senftle T P, Hong S, Islam M M, Kylasa S B, Zheng Y, Shin Y K, Junkermeier C, Engel-Herbert R, Janik M J, Aktulga H M, Verstraelen T, Grama A and van Duin A C T 2016 *The ReaxFF reactive force-field: development, applications and future directions*, *npj Comput. Mater.* **2** (1) 15011
[39] Kittel C 2004 *Introduction to Solid State Physics*, John Wiley & Sons, Inc, **8** 704
[40] González M A 2011 *Force fields and molecular dynamics simulations*, *Collect. SFN* **12** 169
[41] Becker C A, Tavazza F, Trautt Z T, Buarque D M and Robert A 2013 *Considerations for choosing and using force fields and interatomic potentials in materials science and engineering*, *Curr. Opin. Solid State Mater. Sci.* **17** 277
[42] Becker C A and Kramer M J 2010 *Atomistic comparison of volume-dependent melt properties from four models of aluminum*, *Model. Simul. Mater. Sci. Eng.*, IOP Publishing, **18** (7) 74001
[43] van Duin A 2002 *ReaxFF User Manual* 39
[44] Refson K 2001 *Moldy User's Manual*
[45] Ercolessi F 1997 *A molecular dynamics primer*, Spring College in Computatonal Physics
[46] William H, Andrew D and Klaus S 1996 *VMD – Visual Molecular Dynamics*, *Journal of Molecular Graphics* **14** 33
[47] Stukowski A 2009 *Visualization and analysis of atomistic simulation data with OVITO-Open Visualization Tool*, *Modelling and Simulation in Materials Science and Engineering*, IOP Publishing, **18** (1) 15012
[48] *The PyMOL Molecular Graphics System, Version 1.8.* 2015, Schrödinger, LLC
[49] Chapman J B J 2018 *Improving the Functional Control of Ferroelectrics using Insights from Atomistic Modelling*, UCL (University College London)
[50] Leach A R 2001 *Molecular modelling - Principles and Applications*, Prentice Hall

[51] Verlet L 1968 *Computer Experiments on Classical Fluids. II. Equilibrium Correlation Functions*, *Physical Review (Series I)*, The American Physical Society, **165** 201
[52] Allen M P and Tildesley D J 2017 *Computer simulation of liquids*, Oxford University Press
[53] Ciccotti G, Kapral R and Sergi A 2005 *Non-Equilibrium Molecular Dynamics*, Springer Netherlands 745
[54] Tuckerman M E, Liu Y, Ciccotti G and Martyna G J 2001 *Non-Hamiltonian molecular dynamics: Generalizing Hamiltonian phase space principles to non-Hamiltonian systems*, *The Journal of Chemical Physics* **115** (4) 1678
[55] Plimpton S 1995 *Fast Parallel Algorithms for Short-Range Molecular Dynamics*, *Journal of Computational Physics* **117** (1) 1
[56] Aktulga H M, Pandit S A, van Duin A C T and Grama A Y 2012 *Reactive Molecular Dynamics: Numerical Methods and Algorithmic Techniques*, *SIAM J. Sci. Comput.*, Society for Industrial and Applied Mathematics, **34** (1) 1
[57] *LAMMPS Data Format*, *https://lammps.sandia.gov/doc/2001/data_format.html*
[58] *Tryton*, *https://task.gda.pl/kdm/sprzet/tryton-2*
[59] *Strona główna CI TASK*, *https://task.gda.pl*
[60] López H M, Gachelin J, Douarche C, Auradou H and Clément E 2015 *Turning Bacteria Suspensions into Superfluids*, *Phys. Rev. Lett.*, American Physical Society, **115** 28301
[61] Shliomis M I and Morozov K I 1994 *Negative viscosity of ferrofluid under alternating magnetic field*, *Physics of Fluids*, American Institute of Physics, **6** (8) 2855